Forest Ecology and Management 372 (2016) 269–290

Contents lists available at ScienceDirect

Forest Ecology and Management

journal homepage: www.elsevier.com/locate/foreco

Long-term effects of pest-induced tree species change on carbon and nitrogen cycling in northeastern U.S. forests: A modeling analysis

Katherine F. Crowley [a,*], Gary M. Lovett [a], Mary A. Arthur [b], Kathleen C. Weathers [a]

[a] Cary Institute of Ecosystem Studies, Box AB, 2801 Sharon Turnpike, Millbrook, NY 12545, USA
[b] Dept. of Forestry, University of Kentucky, 103 TP Cooper Building, Lexington, KY 40546, USA

ARTICLE INFO

Article history:
Received 10 December 2015
Received in revised form 16 March 2016
Accepted 22 March 2016
Available online 2 May 2016

Keywords:
Invasive pests
Forest ecosystem model
Tree species
Carbon
Nitrogen
Northeastern U.S.

ABSTRACT

Invasive insects and pathogens can cause long-term changes in forest ecosystems by altering tree species composition, which can radically alter forest biogeochemistry. To examine how tree species change may alter long-term carbon (C) and nitrogen (N) cycling in northeastern U.S. forests, we developed a new forest ecosystem model, called Spe-CN, that allows species composition to shift over time. We simulated the effects of species change due to three invaders—beech bark disease (BBD), hemlock woolly adelgid (HWA), and sudden oak death (SOD)—on forest productivity, C storage, and N retention and loss over a 300-year period. The model predicted changes in C and N cycling rates and distribution between vegetation and soils after stands were invaded, with the magnitude, direction, and timing dependent on tree species identity. For a stand in which sugar maple (*Acer saccharum* Marsh.) replaced American beech (*Fagus grandifolia* Ehrh.) due to BBD, the model predicted a change from net C loss (−13% after 100 years) to net C storage (+10% after 300 years), as plant C gain (+36%) overtook C loss from soils (−11%) and downed wood (−24%). Following replacement of eastern hemlock (*Tsuga canadensis* (L.) Carr.) by yellow birch (*Betula alleghaniensis* Britt.) due to HWA, early loss of forest floor C (−28% after 100 years) was exceeded by gain of plant and downed wood C after 145 years; by 300 years, total C differed little between invaded and un-invaded stands. Where red maple (*Acer rubrum* L.) replaced red oak (*Quercus rubra* L.) due to SOD, loss of plant and soil C generated net C loss (−29%) after 100 years that continued thereafter. In contrast to C, for which patterns of storage and loss differed considerably among invasion scenarios, total N was ultimately lower following invasion across all three scenarios. Predicted nitrate leaching was also correspondingly higher in invaded vs. un-invaded stands (+0.3 g m^{-2} $year^{-1}$ of N from nitrate), but the leaching increase lagged by nearly 100 years following HWA invasion. Together, these results demonstrate that the effects of pest-induced tree species change on forest C and N cycling vary in magnitude, direction of effect, and timing of response following invasion, depending on the identity of the declining and replacing species, and that species-specific modeling can help elucidate this variation. Future predictions will need to account for tree species change to generate meaningful estimates of C and N storage and loss.

1. Introduction

Forests of the U.S. have been subject to repeated invasions by destructive insects and diseases imported from other continents, with particular severity in the Northeast (Aukema et al., 2010; Liebhold et al., 2013). As with other disturbances, these pests can produce short-term ecosystem effects due to tree mortality, including reductions in productivity and shifts in nutrient cycling (Loo, 2009; Lovett et al., 2006; Peltzer et al., 2010). Unlike other types of disturbance, however, invasive insects and diseases often target individual tree species, which can change the species composition of the forest. Such shifts in species composition can have long-term implications for forest ecosystems (e.g., Ellison et al., 2005; Lovett et al., 2006).

Replacing one tree species with another can considerably alter key forest ecosystem functions (e.g., Binkley and Menyailo, 2005). Differences among species in growth rate, tissue nitrogen (N) concentrations, allocation to wood, foliage, and roots, litter chemistry, and mycrorrhizal associations cause differences in net primary productivity (NPP), decomposition, soil carbon (C) storage, and N cycling (Finzi et al., 1998; Hobbie, 1992; Lovett et al., 2004).

* Corresponding author.
E-mail addresses: crowleyk@caryinstitute.org (K.F. Crowley), lovettg@caryinstitute.org (G.M. Lovett), marthur@uky.edu (M.A. Arthur), weathersk@caryinstitute.org (K.C. Weathers).

http://dx.doi.org/10.1016/j.foreco.2016.03.045
0378-1127/

Different tree species grown in the same climate and soil conditions can vary in foliar and wood productivity by over 100% (Gower et al., 1993; Reich et al., 2005). Likewise, stands dominated by different species can vary more than 600% in the rate of nitrate (NO_3^-) leaching to surface waters (Lovett et al., 2002), and species-driven differences in net nitrification rates can reach 1000% (Lovett et al., 2004). Carbon and N pools and C:N ratios vary widely in soils under different tree species (e.g., Cools et al., 2014; Ross et al., 2011; Vesterdal et al., 2008), and tree species-specific effects on surface soils extend to soil microbial communities (Scheibe et al., 2015; Urbanova et al., 2015). Loss of a dominant tree species due to an invasive insect or pathogen therefore can have considerable consequences for forest ecosystem functions such as C storage or N retention.

In the northeastern U.S., invasive insects and pathogens are causing, or predicted to cause, declines in several dominant tree species. For example, beech bark disease (BBD) has affected American beech (*Fagus grandifolia* Ehrh.) trees across the northeastern U.S. via the interaction of a scale insect (*Cryptococcus fagisuga*) and fungi of the genus *Neonectria*, beginning in the 1890s (Houston, 1994). Across the region, beech mortality rates have increased and growth rates have declined with time since invasion, despite frequently prolific sprout or seedling regeneration (Morin and Liebhold, 2015). In the Catskill Mountains of southeastern New York, the focal area for our study, decline in beech due to BBD has resulted in a shift toward increasing sugar maple (*Acer saccharum* Marsh.) (Lovett et al., 2010). Sugar maple and beech differ in several plant traits, including lower foliar N and lignin concentrations and more decomposable litter in sugar maple than in beech (Lovett et al., 2013a, 2010, 2004), that strongly influence nutrient cycling processes.

Hemlock woolly adelgid (HWA) is a more recent, insect invader of northeastern U.S. forests that has spread rapidly since the 1950s through the range of eastern hemlock (*Tsuga canadensis* (L.) Carr.), halted in its northward movement by current climatic limits (Trotter and Shields, 2009). In hemlock-dominated stands, hemlock can generate a stable ecosystem with slow decomposition and low rates of N cycling (Ellison et al., 2005; Jenkins et al., 1999). During invasion by HWA, black birch (*Betula lenta* L.) often replaces hemlock in southern New England (Orwig et al., 2002; Stadler et al., 2005), but this pattern is not consistent at the regional scale (Morin and Liebhold, 2015), and yellow birch (*Betula alleghaniensis* Britt.) is a more common associate of hemlock in the Catskills (Lovett et al., 2013b). As with beech and sugar maple, hemlock and birch differ in influential traits such as tissue N concentrations and litter decomposability, which influence C and N cycling in underlying soils (Cobb, 2010; Lovett et al., 2004).

In addition to ongoing invasions, new insects and diseases continue to enter U.S. forests, with new insect arrivals estimated at approximately 2.6 per year (Aukema et al., 2010). Sudden oak death (SOD), a disease caused by the pathogen *Phytophthora ramorum*, has resulted in extensive oak (*Quercus* spp.) mortality in California (Cobb et al., 2012; Rizzo et al., 2005) but has not yet reached the northeastern U.S. Simulation modeling suggests that the invasion is in its early stages and the pathogen is climatically suited to a large area worldwide, including areas of the eastern U.S. where oak species frequently dominate (Ireland et al., 2013). In California, tree species differ in their susceptibility to SOD; thus, in a study of ecosystem effects of SOD, the largest effects on ecosystem processes occurred via changes in species composition, which in turn altered litterfall chemistry, litterfall mass, and soil NO_3^- availability (Cobb et al., 2013). Oak species are frequent dominants in eastern U.S. forests, and habitat suitability for the oak-hickory forest type is predicted to increase in the Northeast as the climate warms (Iverson et al., 2008). If SOD reaches the eastern U.S., it may drive replacement of abundant red oak (*Quercus rubra* L.) by species such as red maple (*Acer rubrum* L.), a common associate of red oak in the Catskill Mountains of New York (Lovett et al., 2013b) but with lower foliar N and lignin concentrations and more decomposable litter.

Given observed variation in species-specific traits and distinctive effects of individual tree species on ecosystem processes, species transitions following disease or insect invasion are likely to have long-term effects on forest C and N cycling. Long tree life spans limit tests of such predictions, however. In the Catskill Mountains, a chronosequence study of stands with increasing BBD invasion demonstrated effects of decreasing beech and increasing sugar maple abundance on C and N cycling over a time scale of approximately 50 years (Lovett et al., 2010). Similarly, studies in central and southern New England have examined impacts of HWA along gradients of increasing hemlock mortality (Jenkins et al., 1999) and increasing successional age following infestation (Finzi et al., 2014; Raymer et al., 2013).

Another approach to the problem of predicting long-term impacts of species change is to use simulation models in which differences in key traits of dominant tree species drive differences in forest C and N cycling over long time scales. Along these lines, Albani et al. (2010) used the Ecosystem Demography (ED) model to simulate HWA effects on C dynamics across the eastern U.S., modifying a late-successional conifer functional type to better represent eastern hemlock; however, ED does not specifically simulate individual species or changing composition within a functional type. Other ecosystem models used extensively in the region (e.g., PnET-CN (Aber et al., 1997; Ollinger et al., 2008) and CENTURY (Parton et al., 1987)) also do not allow species composition to change over time.

Here we present a new forest ecosystem model, Spe-CN, that simulates C and N cycling in single- and mixed-species stands as tree species composition changes, and use the model to predict effects of invasive insects and pathogens on forest ecosystem processes over a period of 300 years. Specifically, we use Spe-CN to simulate changing tree species composition associated with BBD, HWA, and SOD in hypothetical forest stands in the Catskill Mountains of New York, and examine short- and long-term predictions of the effects of these tree species transitions on forest productivity, C storage, and N retention and loss.

2. Materials and methods

2.1. Study area

We developed the Spe-CN model for application to species change scenarios in northeastern U.S. forests. We used field data from across the region to develop and parameterize the model, both to make the model regionally applicable and to improve parameter estimates. To achieve sufficient testing of single-species effects, we tested the model using field data from three sub-regions (Table 1): the Catskill Mountains of New York (Lovett et al., 2013a, 2002, 2004; Templer et al., 2005); the White Mountain National Forest (WMNF) in New Hampshire (Goodale and Aber, 2001; Ollinger et al., 2002); and the Great Mountain Forest (GMF) in Connecticut (Finzi et al., 1998). Tests against field data used versions of the model parameterized with temperature records, N deposition estimates, and foliar N concentrations specific to each sub-region.

To run simulations of species transitions due to BBD, HWA, and SOD, we used the version of the model parameterized for the Catskill Mountains, an area severely affected by invasive forest pests (Liebhold et al., 2013; Lovett et al., 2013b). We ran invasion scenarios for a single focal area to emphasize responses to tree species change, rather than factors such as temperature or N deposition

Table 1
Location, climate, and N deposition for the three sub-regions.

Sub-region[a]	Latitude	Longitude	Elevation	Annual precipitation	Jan. mean temperature	July mean temperature	Peak N deposition	Final N deposition	AB	EH	RM	RO	SM	YB
	(degrees N)	(degrees W)	(m)	(mm)	(deg C)	(deg C)	(g m^{-2} year^{-1} of N)		(Number of plots by species[b])					
Catskills														
Single sp	41.92–42.31	74.10–74.86	320–1232	1482	−6.7	18.0	1.11	0.67	6	6	0	6	6	6
Survey									2	1	4	6	33	13
GMF	42	73.25	300–500	1356	−6.1	20.1	0.97	0.59	12	12	12	12	12	0
WMNF	43.90–44.59	71.11–71.91	300–914	1386	−7.8	18.8	0.68	0.42	3	2	1	0	10	12

[a] Single sp = Catskills single-species plots (Lovett et al., 2013a, 2004; Templer et al., 2005); Survey = Catskills survey plots (Lovett et al., 2002); GMF = Great Mountain Forest (Finzi et al., 1998); WMNF = White Mountain National Forest (Goodale and Aber, 2001; Ollinger et al., 2002). See Sections 2.2 and 2.3 for further details.
[b] AB = American beech; EH = eastern hemlock; RM = red maple; RO = red oak; SM = sugar maple; YB = yellow birch.

that vary across the larger northeastern U.S. region. Tree species in these simulations included American beech, eastern hemlock, red maple, red oak, sugar maple, and yellow birch, which are frequently dominant in northeastern U.S. forests.

2.2. Model structure and parameterization

Our primary objective in developing the Spe-CN model was to predict long-term changes in forest C and N cycling attributable to changes in tree species composition. We include a detailed description of the model as Appendix A; a brief overview is given here. We developed Spe-CN using available field data and field-based empirical relationships wherever possible, and adapted relevant algorithms from ecosystem models such as PnET-CN (Aber and Federer, 1992; Aber et al., 1997) and CENTURY (Parton et al., 1987, 1988) for use in a species-specific context. As with other forest C and N cycling models, Spe-CN incorporates the processes of NPP, tree N uptake, litter production, decomposition, and soil organic matter (SOM) formation (Fig. 1, Appendix A). The Spe-CN model differs from other models primarily by including individual tree species, such that the user can simulate forest stands that change in tree species composition over time. Tree species vary in key plant traits (Tables A.1 and A.2 and outlined below) that differentially influence productivity, nutrient uptake, turnover, and decomposition processes, such that changing species composition will gradually alter C and N cycling on the site. Spe-CN does not model individual trees like the Linkages model (Pastor and Post, 1986), nor does it simulate population demography like the ED model (Albani et al., 2010; Moorcroft et al., 2001). Additionally, Spe-CN does not simulate physiological impacts to specific plant tissues due to insect or disease invasion (Dietze and Matthes, 2014). Rather, Spe-CN simulates pools of C and N in plant structures (foliage, fine wood, coarse wood, roots) for individual species, and plays out the long-term consequences of user-specified trends in species composition for C and N cycling in the forest.

In the Spe-CN model, production and N uptake move C and N into vegetation pools (Fig. 1, Appendix A). Turnover of foliage, roots, fine wood, and fragmented coarse wood moves plant material into the litter and subsequently the humus pool, which together are considered to make up the forest floor or O horizons.

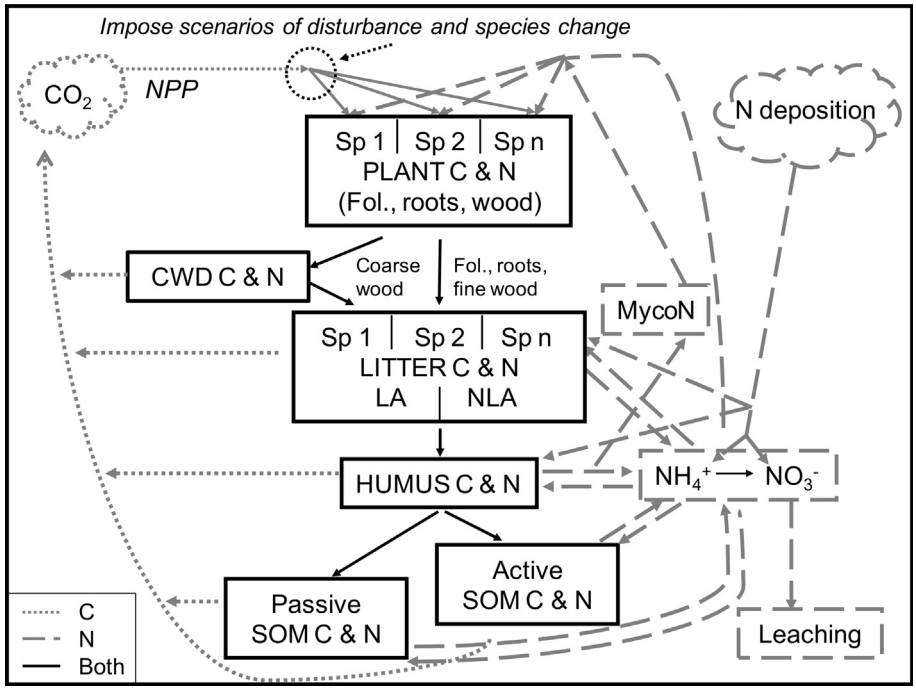

Fig. 1. Structure of the Spe-CN forest ecosystem model. Dotted, dashed, and solid lines show movement of C, N, or both C and N, respectively. Carbon and N move among pools in the atmosphere, vegetation (species-specific foliage, root, fine wood, and coarse wood pools), coarse woody debris (CWD), forest floor (litter and humus), and upper mineral soil (active and passive SOM). Mineralized N may be immobilized in soil, moved into a mycorrhizal N pool (MycoN), taken up by plants, or nitrified; NO_3^- leaches out of the system if not taken up by vegetation. Sp = species; LA = lignin-associated; NLA = non-lignin-associated. Controls on process rates, movement between pools, and other model details are discussed in Appendix A.

Unfragmented CWD decomposes in a separate pool. A fraction of the humus pool is transferred to active and passive SOM pools in the mineral soil, which represent the surface mineral soil to a depth incorporating most root uptake. Nitrogen mineralized from organic or mineral soil pools or the CWD pool may be nitrified, as a function of soil C:N (Lovett et al., 2004) and plant demand for N (Aber et al., 1997); immobilized in soil; moved into a mycorrhizal N pool to contribute to plant N uptake; or moved into inorganic soil ammonium (NH_4^+) pools available for direct plant uptake. Soil NO_3^- is also available for plant uptake, and any remaining NO_3^- leaches from the system (Fig. 1, Appendix A). In the current version of the model, the only N loss from the system is NO_3^- leaching; dissolved organic N (DON) leaching and denitrification are not simulated. Leaching of DON is a minor N loss mechanism for most watersheds in our focal study area of the Catskill Mountains (Lovett et al., 2000), although denitrification may be important in some locations (e.g., Morse et al., 2015). Adding denitrification to the model will require development of a hydrologic submodel that determines soil saturation. For the current model version, we assume that denitrification is unlikely to be an important flux in our study area's aerobic, well-drained soils, while acknowledging that the model may overestimate NO_3^- leaching somewhat due to the lack of gaseous N losses.

Spe-CN differs from other forest ecosystem models in that many of the processes transferring C and N among vegetation and soil pools are governed by species-specific traits. Key parameters include minimum and range of N concentrations in foliage, fine wood, coarse wood, and roots; foliar turnover; allocation to foliage vs. wood; fraction of N resorbed from foliage before litterfall; tissue lignin and cellulose concentrations; the slope of the relationship between litter N concentration and mass loss (N mass loss or NML; Aber et al., 1990); and maximum biomass attainable in pure stands (Tables A.1 and A.2). Foliar N concentration determines NPP, based on empirical relationships between canopy N and aboveground NPP (ANPP) for gymnosperm and angiosperm tree species (Smith et al., 2002). Foliar N varies within a species-defined range in response to N availability. Allocation to wood vs. foliage is also a function of foliar N for angiosperms (Smith et al., 2002), and root allocation differs for gymnosperm vs. angiosperm species (Nadelhoffer and Raich, 1992). Nutrient uptake from the soil is determined by growth, tissue N concentrations, and N availability from inorganic soil NH_4^+ or NO_3^- pools. Nitrogen taken up by the plant is stored as "mobile" N within the coarse and fine wood tissues and used to support production (e.g., Millard and Grelet, 2010).

Species-specific traits influence litterfall and decomposition as well as production. Foliar turnover differs for gymnosperm and angiosperm species, influencing the nutrient content of material entering the forest floor, and root turnover is a function of available soil N (Aber et al., 1985). The fraction of N resorbed from foliage before litterfall is species-specific, and resorbed N moves into a bud N pool that combines with mobile N to support the following year's NPP. Litter from foliage, roots, fine wood, and fragmented coarse wood immobilizes or mineralizes N according to species- and tissue-specific empirical relationships between litter N concentration and mass loss (NML; e.g., Aber et al., 1990; Appendix A). Fresh litter is divided into lignin-associated (lignin plus cellulose) and non-lignin-associated pools based on tissue lignin concentration and the lignin:N ratio for each species (Parton et al., 2007, 1988), and decomposes in these pools within each of three litter cohorts. Litter transfers from one cohort to the next at the end of each growing season (Appendix A), and together the three litter cohorts represent the period during which N immobilization may occur in the litter, as determined from the NML relationship. For a mixed-species stand, the total extent of litter decomposition is ultimately calculated as a weighted average for the species present. The oldest litter cohort moves into the humus pool each year, where decomposition rates vary between gymnosperm and angiosperm species (Olsson et al., 2012; Vesterdal et al., 2012). By the time material is transferred to the active and passive SOM pools, species composition no longer influences decomposition rates, due to lack of data to describe or parameterize differences among species for these pools.

Tree species composition also influences N mineralization and nitrification. Nitrogen mineralization from the humus, active and passive SOM, and CWD pools is a function of C mineralization modified by the ratio of net to gross N mineralization (NGR), which defines the fraction of the mineralized N that moves to soil available NH_4^+ or (following nitrification) NO_3^- pools. The humus NGR is lower for soils underlying arbuscular mycorrhizal (AM) than ectomycorrhizal (EM) tree species, based on the assumption that AM fungi are poorer competitors with heterotrophic soil microbes, thereby resulting in greater soil N retention in AM- than EM-dominated stands (Langley and Hungate, 2003). A greater fraction of N mineralized from the humus moves into a mycorrhizal N pool when EM species dominate the stand, and this mycorrhizal N is allocated among tree species based on mycorrhizal status (EM species receive a greater fraction than AM species (Langley and Hungate, 2003)) and relative N demand by tree species. Together, these algorithms reflect differences in an AM vs. EM nutrient economy (Averill et al., 2014; Langley and Hungate, 2003; Phillips et al., 2013). Spe-CN simulates nitrification as a function of soil C:N (Lovett et al., 2004), which varies with the dominant tree species. Nitrification rate is also influenced by overall plant demand for N, which is a function of current plant N relative to the maximum possible plant N at the current biomass; this assumes that plants compete more strongly for NH_4^+ relative to nitrifiers when plant N demand is high (Aber et al., 1997). Ultimately, the amount of NO_3^- leached reflects cumulative species-specific effects on C and N cycling processes.

Before running a scenario in the Spe-CN model, the user can specify several site-specific factors that will influence C and N cycling, including tree species composition, type and rate of species change, disturbance history, N deposition regime, mean monthly temperature, and the first and last months of the growing season. To set a disturbance regime (e.g., harvest, fire, etc.), the user specifies the year and month of each disturbance, the fraction of the forest floor lost due to the disturbance, the fraction of biomass killed for each species present, and the fraction of the aboveground biomass removed from the site (also by species). This disturbance simulator is very similar to the approach used in the PnET model (Aber and Driscoll, 1997; Aber et al., 1997). For N deposition, the user specifies the total (wet plus dry) deposition at up to three time steps, and the model interpolates values between these points. Spe-CN then distributes the added N between the organic N and inorganic NO_3^- or NH_4^+ pools in the litter and humus (Appendix A).

Mean monthly temperature influences decomposition rates in the litter, humus, active SOM, and CWD pools, using a decomposition modifier developed for PnET (Aber et al., 1997; Appendix A), and growing season length constrains plant growth and N uptake. For this analysis, the first and last months of the growing season were set to May and October, reflecting average conditions for the region. To estimate mean monthly temperature for each subregion, we calculated 30-year averages of monthly mean temperature values (Table 1). Catskills estimates were from Slide Mountain, NY (GHCND: USC00307799, 1981–2010) and East Jewett, NY (GHCND: USC00302366, 1985–2015) stations, using data downloaded from NOAA NCDC Climate Data Online (https://www.ncdc.noaa.gov/cdo-web/). Great Mountain Forest estimates were from Norfolk, CT (GHCND:USC00065445, 1981–2010). White Mountain National Forest temperature estimates were derived

from Station 1 from the Hubbard Brook Ecosystem Study (1981–2010; Campbell and Bailey, 2015a,b). We ran simulations under an average temperature regime (varying by month, but consistent from year to year) in order to emphasize changes in C and N cycling driven specifically by tree species.

We used trends of N deposition approximating the patterns observed in precipitation monitoring data. For each sub-region, total (wet plus dry) N deposition was held constant at a baseline of 0.2 g m^{-2} $year^{-1}$ of N until 1940, increased to a maximum value by 1990, and decreased to a mean 2010 value based on NADP and CASTNET data (Table 1; http://java.epa.gov/castnet/clearsession.do). We used maximum N deposition estimates for the Catskills and WMNF from Lovett and Rueth (1999), and for GMF from the Catskills (Lovett and Rueth, 1999) and Abington, CT (CASTNET ABT147) as the nearest available sites. Nitrogen deposition estimates for 2010 were averages from 2007 to 2013 of available NADP NTN (NY68, NH02, ABT147) and CASTNET (CAT175, ABT147, WST109) data totaling wet plus dry deposition. For the WMNF, dry deposition estimates from WST109 (Woodstock, NH, elevation 255 m) were multiplied by 3.5 to adjust to the higher mean elevation of WMNF sites, per the relationship between dry deposition estimates from low (250 m) vs. high (650 m) elevation sites observed at Hubbard Brook (Lovett et al., 1997).

The model operates on a monthly time step, and we programmed the model in Visual Basic for Applications within Microsoft Excel to make the code easily accessible. Further specifics regarding the model's algorithms and parameters are included in Appendix A.

2.3. Model testing

We tested the ability of the Spe-CN model to simulate the effects of pest-induced changes in tree species composition in two ways. First, we compared Spe-CN simulations of key C and N cycling variables to field data from plots located in three sub-regions across the northeastern U.S. and dominated by one of six tree species used in our simulations. Second, we simulated the C:N ratio in the Oe + Oa (henceforth referred to as OeOa) horizons of the forest floor for a chronosequence of plots reflecting a BBD-induced shift in dominance from beech to sugar maple in the Catskill Mountains of New York (Hancock et al., 2008; Lovett et al., 2010).

To test the Spe-CN model for application to stands dominated by sugar maple, beech, yellow birch, hemlock, red oak, or red maple, we compared modeled values to independent field data (not used to parameterize the model) from plots in the Catskill Mountains (Lovett et al., 2002, 2004, 2013a; Templer et al., 2005), the WMNF (Goodale and Aber, 2001; Ollinger et al., 2002), and the GMF (Finzi et al., 1998; Table 1). Data from the Catskills were derived from two sources, a long-term N addition study in plots dominated by single species (Lovett et al., 2004, 2013a; Templer et al., 2005) and a broader survey of mixed-species plots across the region (Lovett et al., 2002). For WMNF and Catskills mixed-species plots, we defined a species-dominant plot as having a minimum of 50% relative basal area of the target species, although in most cases relative basal area exceeded 70%. The GMF plots were focused around individual trees, and thus represent single-species plots.

To test the model's ability to distinguish species-specific effects, we used versions of Spe-CN parameterized with mean monthly temperature, N deposition, minimum foliar N concentration, and foliar N range for each sub-region to simulate C and N pools and process rates for second- and old-growth stands dominated by each species. Second-growth stands were simulated at 90 years post-disturbance, which is the approximate age of field plots with known land-use history; old-growth stands were simulated at 300 years, to approximate the age of field plots labeled as old-growth. Tests of the model's ability to simulate old-growth conditions could not be as thorough as for second-growth forest, however, due to the small number of available species-dominant field plots from older forests. We plotted the field data and the range in Spe-CN modeled values for each output variable across the test areas, by species, such that the Spe-CN simulations reflected the range of temperature, N deposition, and stand ages represented by the field data. Thus, the model output represents an average condition for each species. It is important to note that the model emphasizes differences attributable to the dominant tree species, and does not attempt to capture variability due to site-specific characteristics such as soil texture, water status, or unknown aspects of site history; similarly, it does not simulate changes in climate over time.

Available field data for this analysis included the C and N pools and C:N ratios for the OeOa horizons in the forest floor (available for all three sub-regions); wood C, foliar N, and the ratio of nitrification to N mineralization (i.e., nitrification fraction) in the OeOa (available for the Catskills and WMNF); and aboveground NPP (ANPP; available for Catskills only). While the Spe-CN model does not specifically simulate depth profiles in the soil, for testing purposes we assumed that the model's litter and humus pools, minus the upper two litter cohorts, constitute the Oe + Oa horizons in the forest floor that are typically sampled in the field. We did not test the model against field data on mineral soil pools because the model does not specify a depth or horizon structure for the mineral soil. Model estimates of total soil C were within an appropriate range for northeastern U.S. forests (Fahey et al., 2005; Johnson, 2013; McFarlane et al., 2013), however, so we considered broad predicted patterns in total soil C and N to be reasonable.

In the available field data, stands dominated by different tree species differed significantly in measures of C and N cycling within a sub-region (Lovett et al., 2004, 2013a; Finzi et al., 1998). While variation was high across the three sub-regions, the Spe-CN model captured the pattern of the mean differences among species present in the field data; the range in simulated values typically fell within two standard errors of the mean of field data from the Catskills, WMNF, and GMF (Figs. 2, 3 and B.1). As expected, site-level exceptions appeared to derive from unusual site characteristics or land use history not typical of the testing data set as a whole. Further details are provided in Appendix B.

Field data and model simulations had the best correspondence for plant and soil C and N pools, including OeOa C, N, and C:N and wood C (Fig. 2, Appendix B). For ANPP, field data were limited, but Spe-CN modeled values were in general agreement with the available Catskills data except for yellow birch; the model's overestimation of yellow birch ANPP appeared to result from the fact that Catskills yellow birch stands are often underlain by thin soils on a rock substrate, which is not captured in the model (Fig. 3, Appendix B). For the nitrification fraction for the OeOa horizons in the forest floor, the Spe-CN model captured the pattern observed among tree species in the Catskills (i.e., maple > beech, yellow birch > hemlock, red oak; Lovett et al., 2004). The model simulations underestimated the magnitude of the nitrification fraction for Catskills sugar maple and beech plots, but corresponded well to WMNF estimates (Appendix B; Goodale and Aber, 2001; Ollinger et al., 2002).

To test the model's ability to predict the effects of changes in tree species composition due to invasive pests, we compared model simulations of OeOa C:N to Catskills field data from a chronosequence of plots invaded by BBD, including plots dominated by beech and sugar maple as the end members (Hancock et al., 2008; Lovett et al., 2010, 2004; Templer et al., 2005). Along this BBD gradient, the Spe-CN model simulated the pattern of decreasing OeOa C:N with increasing sugar maple abundance

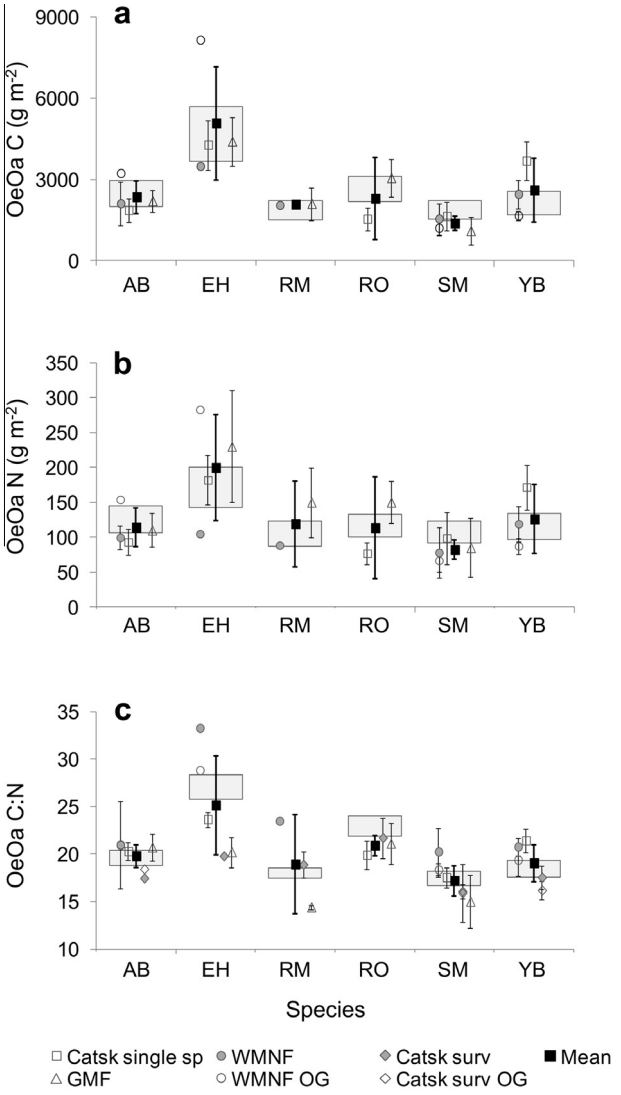

Fig. 2. Comparison of Spe-CN model simulations to field data from plots dominated by single species for OeOa horizons in the forest floor, including (a) OeOa C, (b) OeOa N, and (c) OeOa C:N. On each plot, the bars provide the range of Spe-CN modeled values across N deposition, temperature, and stand ages associated with field data from the Catskills, WMNF, and/or GMF. Points give the mean value ±2 standard errors for field data within each sub-region and across the three sub-regions (labeled as "Mean"). The mean values across sub-regions indicate the extent of overlap with model predictions, and also provide a broad assessment of regional variability for each species. Significant differences among species for each variable are reported in the original studies (Lovett et al., 2004, 2013a; Finzi et al., 1998). Field data indicated as "OG" are from old-growth forest, simulated at 300 years post-disturbance; other field data are from second-growth forest, simulated at 90 years. AB = American beech; EH = eastern hemlock; RM = red maple; RO = red oak; SM = sugar maple; YB = yellow birch.

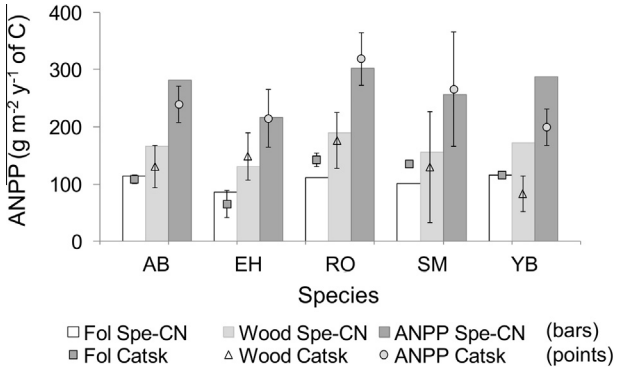

Fig. 3. Comparison of Spe-CN model simulations to field data from Catskills plots dominated by single species for foliar, wood, and total aboveground NPP (ANPP). Bars provide Spe-CN modeled values for each species, and points give the mean value ±2 standard errors for Catskills field data. AB = American beech; EH = eastern hemlock; RO = red oak; SM = sugar maple; YB = yellow birch.

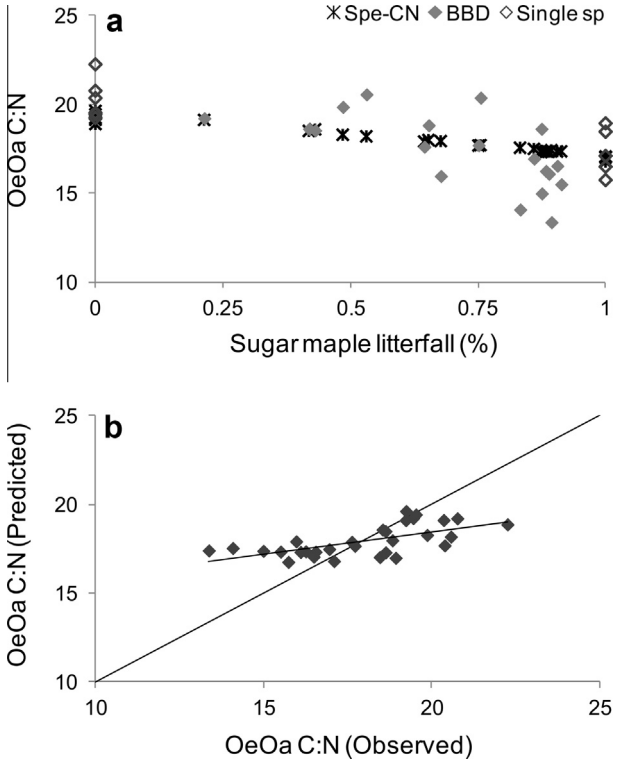

Fig. 4. Comparison of Spe-CN model simulations of C:N for OeOa horizons in the forest floor to field data from plots with decreasing beech and increasing sugar maple abundance. Estimates of OeOa C:N are plotted (a) as a function of sugar maple abundance, and (b) as observed values vs. values predicted by the model. Data are from plots dominated by beech or sugar maple (labeled "single sp"; Lovett et al., 2004; Templer et al., 2005) and from a chronosequence of plots with increasing damage by BBD (labeled "BBD"; Hancock et al., 2008; Lovett et al., 2010).

observed in the field data (Fig. 4a), and the relationship between observed and predicted values of OeOa C:N was strongly linear ($p < 0.001$; Fig. 4b). The slope of this relationship was less than one (Fig. 4b), mainly because the model did not capture the wide variability in OeOa C:N in sugar maple plots, where OeOa C:N can be very low in field measurements (Fig. 4). This suggests that the model provides a conservative estimate of changes in soil C:N associated with this species transition, and other mechanisms beyond those currently included in the model may influence soil C:N at specific sites.

Overall, results from model testing against plots dominated by single species and a BBD chronosequence indicate that we can apply Spe-CN effectively to landscape-level questions (e.g., over tens to hundreds of square kilometers) to evaluate the mean effects of changing tree species composition on forest C and N cycling. At the site level (e.g., less than one to tens of square kilometers), model simulations of mean species effects did not capture the full extent of site-specific variability within a species. Site-level application thus would require further model development to address additional drivers of ecosystem processes such as variations in land use history, soil texture, and other site-specific characteristics that influence forest C and N dynamics beyond the effects of tree species. Limitations and future directions for the Spe-CN model are discussed in detail in Section 4.4.

2.4. Sensitivity analysis for parameter estimates

We performed a sensitivity analysis on the full set of parameters employed in the model (Tables A.1 and A.2) to assess the magnitude of change that a 20% increase or decrease in each parameter would generate in key output variables, with all other parameters held constant (Appendix C). Changes in most parameters had a small effect (<10% change) on most of the output variables considered (NPP; plant C; plant N; OeOa C, C:N, and nitrification rate; and NO_3^- leaching). The output variable with the greatest sensitivity to changes in parameter values was OeOa nitrification, which was the only variable to show a large response (>30%) to a 20% change in some parameter values. This sensitivity to multiple model parameters reflects the dependence of nitrification rate on the outcome of numerous other interacting processes related to both vegetation and soils. Detailed output and discussion of the sensitivity analysis of model parameters are included in Appendix C.

2.5. Invasion scenarios

We used the Spe-CN model to simulate changes in tree species composition caused by three forest insect and disease invasions observed or predicted to occur within the Catskill Mountains of New York—specifically, BBD, HWA, and SOD. For each simulation, we used known forest history for the Catskill Mountains (Kudish, 1979) to set a disturbance regime that would establish an appropriate starting condition for the stand, including forest age and associated C and N pools in vegetation and soils. We then used Spe-CN to predict effects of pest-induced shifts in dominant tree species on C and N cycling. Because our objective was to isolate the effects of changes in species composition, we did not simulate specific forest management responses to invasion, such as salvage logging, that would interact with tree species change to influence C and N dynamics. In these model runs, the dynamics of the disease-causing organism are not specifically modeled; rather, the disease impact is simulated via the tree species replacements, by decreasing production and plant pools of C and N for the host tree species over a specified transition period, and simultaneously increasing production and pools of the replacing tree species. We performed simulations of the following hypothetical scenarios:

1. BBD: The starting condition was a stand of 80% beech and 20% sugar maple harvested in 1910 (80% harvest, 90% removal of aboveground biomass, 10% forest floor loss) following a spin-up period from year 0. Beech bark disease was set to invade the second-growth beech-sugar maple stand in 2020, such that sugar maple replaced beech over a 50-year transition period.
2. HWA: The starting condition was a stand of 80% hemlock and 20% yellow birch disturbed in 1850 by the tanbark industry (100% mortality of hemlock with 10% removal of biomass, no mortality of birch, 5% forest floor loss). Hemlock woolly adelgid was set to invade the second-growth hemlock-birch stand in 2020, such that yellow birch replaced hemlock over a 30-year transition period.
3. SOD: The starting condition was a stand of 80% red oak and 20% red maple harvested in 1910 (80% harvest, 90% removal of aboveground biomass, 10% forest floor loss). Sudden oak death was set to invade the second-growth oak-red maple stand in 2020, such that red maple replaced oak over a 20-year transition period.

We reiterate that these scenarios are hypothetical and are intended to allow us to compare pest impacts; in reality BBD is already distributed throughout the Catskills, HWA is spreading through the region currently, and SOD has not yet reached the area (Lovett et al., 2013b).

2.6. Analysis

In addition to the three species transition scenarios, we also extended the simulations of the original three hypothetical stands in the absence of invasion. We then compared model predictions of C and N pools and process rates between invaded and un-invaded forest stands 100 and 300 years following invasion, to assess potential short- and long-term changes in C and N cycling due to species replacement. Comparing invaded and un-invaded stands in this way allows us to distinguish the invasion effect from other ongoing changes in the forest, particularly the recovery from past disturbances and responses to recent changes in atmospheric N deposition. While it is rare for northeastern U.S. forests to reach 300 years without major disturbance, we extended simulations over this time period both to illustrate that response patterns can change substantially as the forest ages, and to investigate if and when major shifts in C and N cycling could result from species change.

Specifically, we compared predictions of NPP, NO_3^- leaching, plant C and N, downed wood C and N, and soil C and N between invaded and corresponding un-invaded stands with the same history apart from invasion. For soil pools, we evaluated differences both in the forest floor (litter plus humus), where the largest effects on soils occurred; and in the total soil pools (forest floor plus mineral soil), in order to assess net predicted changes in total soil C and N. Predicted trends were comparable for the OeOa horizons (simulated as the forest floor minus the most recent two years of surface litter) vs. the total forest floor C and N pools. Therefore, we used the OeOa as a surrogate for the total forest floor pools, in order to present model predictions as comparable as possible to field measurements from stands of similar history. Finally, net predicted changes in total C and N for a forest stand were assessed across total plant, downed wood, and soil pools.

3. Results

3.1. Beech bark disease

With replacement of beech by sugar maple due to BBD, the Spe-CN model predicted a change in distribution of C between vegetation and soil pools following invasion, accompanied by a transition from net C loss to net C storage. During and immediately following the transition from beech to sugar maple, the model predicted smaller C pools in the vegetation and then in the forest floor; this was due to the slow increase in sugar maple biomass relative to the rapid loss of mature beech, in combination with faster litter decomposition in the new sugar maple stand (Fig. 5a). The decrease in plant and forest floor C was larger in magnitude and duration than the short-term increase in downed wood C resulting from beech mortality (data not shown). Thus, 100 years after the invasion began, the model predicted that total C would be 13% lower (-3.3 kg m^{-2} of C) in an invaded than a corresponding un-invaded stand (Fig. 6a, Table 2). In contrast, for a 300-year-old stand, Spe-CN predicted a transition to greater total C in the replacement sugar maple stand than in an un-invaded beech stand (+10%; +2.8 kg m^{-2} of C), as plant C gain (+36%) overtook C loss from soils (-11%) and downed wood (-24%; Fig. 6b, Table 2).

In contrast to C, predicted trends in N storage were similar in direction between a 100- and a 300-year-old stand. As for C, the model predicted a decline in N pools following invasion, first in vegetation and then in the forest floor, but for N the decline persisted over time (Fig. 5b). By 300 years after the invasion began, total N remained lower in the sugar maple stand than in the un-invaded beech stand (-4%) due to lower maple tissue N

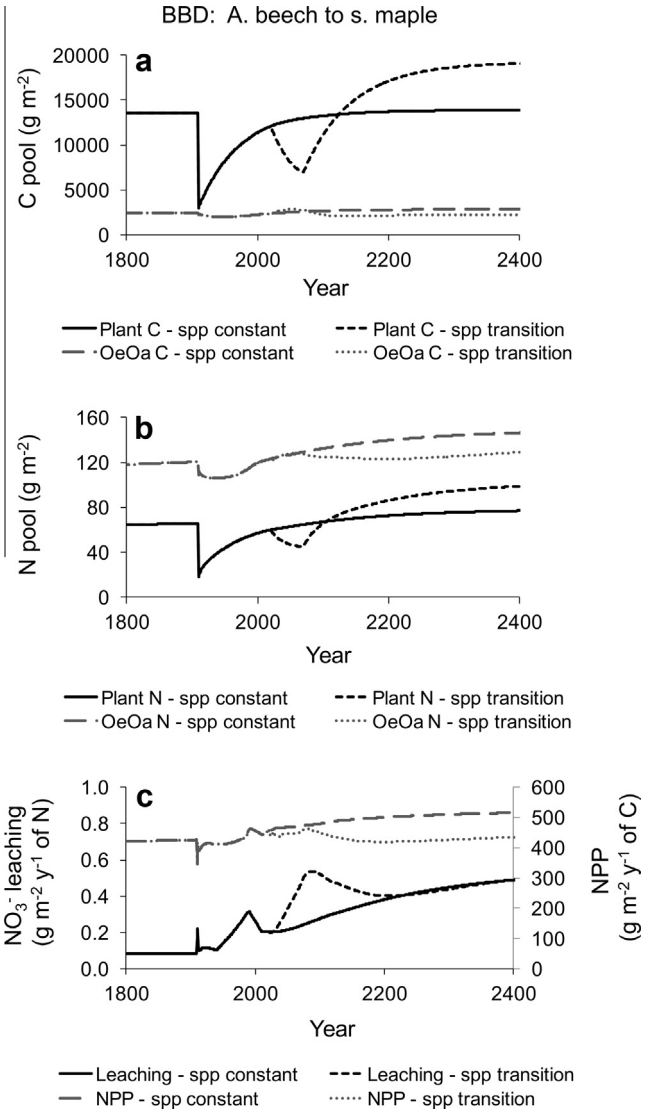

Fig. 5. Comparison of Spe-CN model predictions of (a) C pools in vegetation and OeOa horizons of the forest floor, (b) N pools in vegetation and OeOa horizons of the forest floor, and (c) NPP and NO_3^- leaching between an un-invaded American beech stand and a stand where sugar maple replaces beech due to invasion of BBD. Changes over time are in response to an 80% harvest in 1910; an increase in N deposition from 0.2 to 1.11 g m^{-2} $year^{-1}$ of N from 1940 to 1990, decreasing to 0.67 g m^{-2} $year^{-1}$ of N by 2010 (Table 1); and a transition from beech to sugar maple from 2020 to 2070.

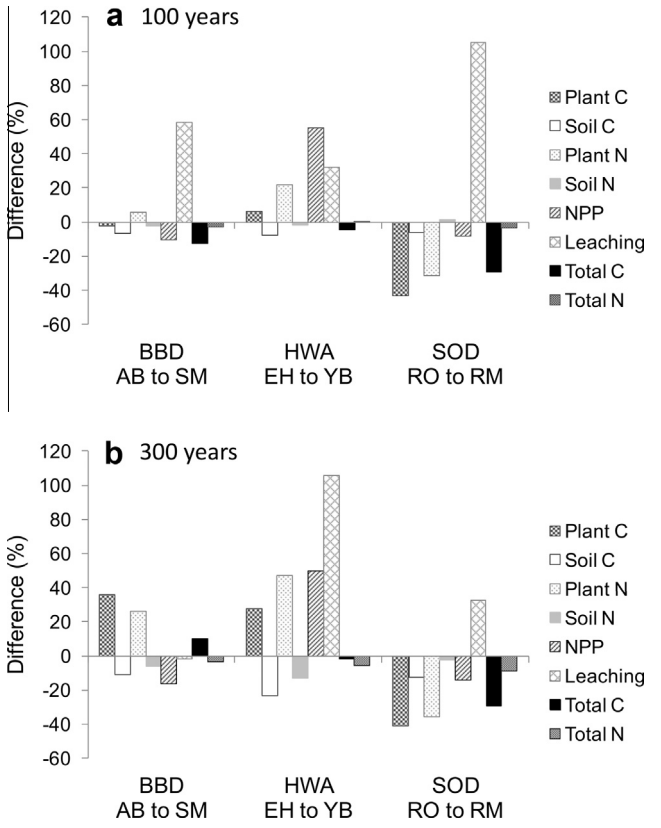

Fig. 6. Predicted differences in C and N pools and process rates between invaded and un-invaded forest stands (a) 100 years and (b) 300 years after the beginning of simulated species transitions due to BBD, HWA, and SOD. Variables include total plant C and N, total soil C and N (forest floor and mineral soil), total C and N (including plant, downed wood, and soil pools), leached NO_3^-, and net primary productivity (NPP). AB = American beech; SM = sugar maple; EH = eastern hemlock; YB = yellow birch; RO = red oak; RM = red maple.

concentrations, a smaller downed wood N pool (−30%), and smaller total N pools in the soil (−6%; Fig. 6b, Table 2).

Corresponding to differences in C and N pools, Spe-CN also predicted shifts in C and N cycling rates associated with the change in species composition. Total NPP was 16% lower in a 300-year-old sugar maple stand relative to an un-invaded beech stand (Fig. 5c, Table 2). Predicted NO_3^- leaching increased by 111% to a peak immediately following the invasion (Fig. 5c) due to N loss from downed wood combined with insufficient N storage in soils or vegetation in the young sugar maple stand. By 300 years post-invasion, however, NO_3^- leaching was similar in the invaded vs. un-invaded stands (Figs. 5c and 6b, Table 2).

3.2. Hemlock woolly adelgid

With replacement of hemlock by yellow birch due to HWA, the Spe-CN model predicted an altered distribution of C between soil and plant pools, but there was little net difference in total C in an invaded vs. an un-invaded stand by 300 years following invasion. The pattern of net storage or loss of C during species replacement and stand recovery was driven by loss of hemlock and subsequent recovery of yellow birch, accompanied by an overall decline in the forest floor and therefore total soil C pool over time (Fig. 7a, Table 2). One hundred years after the invasion began, the model predicted lower total C (−5%; −1.5 kg m^{-2} of C) in an invaded relative to an un-invaded stand primarily due to lower C in forest floor (−28%) and downed wood pools (−24%), which received an initial pulse of wood with hemlock mortality but subsequently declined due to low wood turnover in the young birch stand (Figs. 6a and 7a, Table 2). By 145 years post-invasion, C pools were larger in the invaded than in the un-invaded stand as growth of yellow birch and corresponding recovery of downed wood C pools outstripped soil C losses (data not shown). Ultimately, however, continued loss of forest floor C due to greater decomposition rates in the yellow birch stand and a leveling-off of yellow birch biomass (Fig. 7a) resulted in slightly lower total C (−2%; −0.6 kg m^{-2} of C) in the yellow birch stand relative to an un-invaded hemlock stand by 300 years post-invasion (Fig. 6b, Table 2).

For N, the yellow birch stand transitioned from net storage to net loss (relative to an un-invaded hemlock stand) approximately 100 years post-invasion (Figs. 6a and 7b, Table 2). By 300 years following the invasion, N was 6% lower in the invaded stand (Fig. 6b), primarily due to smaller forest floor N pools (−27%) in a stand dominated by yellow birch (Table 2).

Table 2
Spe-CN model predictions of C and N pools and process rates for invaded vs. un-invaded stands, for each invasion scenario, after 100 and 300 years.

Invasion scenario[a]	Stand age[b]	Plant C	Downed wood C	Soil C[c]	Total C[d]	Plant N	Downed wood N	Soil N[c]	Total N[d]	OeOa C[e]	OeOa N[e]	OeOa C:N[e]	NPP	OeOa Nitrif.[e]	OeOa N Min.[e]	Leached NO_3^-–N
	(years)	($g\ m^{-2}$ of C or N)												($g\ m^{-2}\ year^{-1}$ of C or N)		
BBD																
AB	100	13,394	3932	9259	26,585	68	29	481	578	2701	134	20	486	0.3	5.4	0.3
AB to SM	100	13,060	1559	8624	23,243	72	19	469	561	2124	124	17	437	1.2	4.6	0.5
AB	300	13,866	4445	9902	28,213	76	37	520	633	2844	145	20	511	0.7	5.7	0.5
AB to SM	300	18,800	3371	8801	30,972	96	26	488	610	2240	126	18	428	0.9	4.6	0.5
HWA																
EH	100	12,214	4285	16,125	32,624	62	24	640	726	4478	175	26	340	0.1	3.1	0.2
EH to YB	100	12,976	3263	14,842	31,081	75	25	627	727	3230	160	20	527	0.5	5.8	0.3
EH	300	12,394	4860	17,714	34,967	67	29	712	808	5062	199	25	371	0.1	3.5	0.3
EH to YB	300	15,833	4933	13,583	34,350	99	44	619	762	2700	145	19	556	0.9	6.0	0.6
SOD																
RO	100	17,964	3497	9529	30,990	88	26	434	548	2779	121	23	461	0.2	4.8	0.2
RO to RM	100	10,246	2751	8919	21,916	60	27	441	529	2201	125	18	424	1.2	4.5	0.5
RO	300	18,696	4242	10,407	33,345	101	37	480	618	3075	137	22	495	0.4	5.3	0.4
RO to RM	300	11,056	3536	9077	23,668	64	30	470	564	2284	127	18	425	1.2	4.5	0.5

[a] BBD = beech bark disease, HWA = hemlock woolly adelgid, SOD = sudden oak death; AB = American beech, SM = sugar maple, EH = eastern hemlock, YB = yellow birch, RO = red oak, RM = red maple.
[b] Stand age indicates the number of years following the beginning of the simulated invasion by BBD, HWA, or SOD.
[c] Soil C and N include forest floor (litter and humus) and mineral soil (active and passive SOM) pools.
[d] Total C and N are summarized across plant, downed wood, and soil pools.
[e] OeOa horizons represent the forest floor minus the most recent two years of surface litter.

With a transition from hemlock to yellow birch the Spe-CN model predicted increases in both NPP and NO_3^- leaching, but these increases were staggered in time (Fig. 7c). Net primary productivity increased rapidly with the increase in yellow birch and decline of hemlock, and remained high through the remainder of the model run (+50% after 300 years; Figs. 6b and 7c, Table 2). Increases in predicted NO_3^- leaching following the species transition reflected the reduction in forest floor N pools in the new yellow birch stand relative to an undisturbed hemlock stand. The leaching increase was delayed relative to the species transition due to higher soil C:N in the hemlock stand, which initially inhibited nitrification in the model and therefore leaching (Appendix A). After the species transition, additions of high-N yellow birch litter lowered soil C:N in the new birch stand, and nitrification rates therefore increased. The Spe-CN model predicted a 578% increase in forest floor nitrification and 106% increase in NO_3^- leaching for a 300-year-old yellow birch stand relative to an un-invaded hemlock stand (Figs. 6b and 7c, Table 2).

3.3. Sudden oak death

In contrast to the BBD and HWA scenarios, with replacement of red oak by red maple due to SOD, the Spe-CN model predicted reductions in total C storage throughout most of the period following invasion. Large additions of red oak wood and fine litter increased downed wood and forest floor C pools temporarily following the invasion, but low biomass of red maple relative to red oak and rapid decomposition in the new red maple stand caused total C to fall rapidly below that of a corresponding un-invaded red oak stand. By 100 years post-invasion, C was lower across plant (−43%), downed wood (−21%), and soil (−6%) pools, and total C remained 29% lower ($-9.7\ kg\ m^{-2}$ of C) in a red maple stand than an un-invaded red oak stand by 300 years following the invasion (Figs. 6b and 8a, Table 2).

Predicted patterns in N storage were similar to those for C; total N was lower in a red maple stand than in an un-invaded red oak stand at both 100 (−4%) and 300 years (−9%) post-invasion (Fig. 6, Table 2). One hundred years post-invasion, downed wood N and total soil N were slightly higher (+5 and +2%, respectively) in the new red maple stand than in an un-invaded oak stand, but considerably lower plant N in the red maple stand (−31%) resulted in a smaller total N pool (Table 2). By 300 years post-invasion, predicted N was lower in the red maple than the oak stand across all storage pools (Figs. 6b and 8a and b, Table 2).

Predicted effects of a transition from red oak to red maple on NPP and leaching were initially similar in direction and magnitude to those predicted for a transition from beech to sugar maple. Spe-CN predicted lower NPP over time (−14% by 300 years post-invasion) and an immediate increase in NO_3^- leaching (maximum +135% relative to an un-invaded stand) following the SOD invasion (Figs. 6 and 8c, Table 2). Unlike the beech–sugar maple transition, however, leaching was predicted to remain higher over time in a red maple stand than in an un-invaded red oak stand, remaining 33% higher 300 years after the beginning of the invasion (Fig. 6b, Table 2).

3.4. Summary of differences among invasion scenarios

While the model predicted net loss of C across all three invasion scenarios 100 years following invasion, the magnitude of the response varied by scenario (net C loss for SOD > BBD > HWA after 100 years; Fig. 6a). Additionally, when simulations were extended to 300 years, both magnitude and direction of predicted C storage vs. loss differed among the three types of species transition, demonstrating increasing divergence among scenarios over time (SOD, net C loss; HWA, little change; BBD, net C gain after 300 years; Fig. 6, Table 2). Net differences in N retention among scenarios were of lower magnitude than for C. The model predicted net loss of N from invaded relative to un-invaded stands beginning shortly after invasion, with the exception of the hemlock-birch transition, for which net N loss was delayed approximately 100 years.

Among the three invasion scenarios, predicted increases in NO_3^- leaching in invaded relative to corresponding un-invaded stands were of similar magnitude (approximately $0.3\ g\ m^{-2}\ year^{-1}$ of NO_3^-–N) but differed considerably in the timing of the leaching peak. Transitions from beech or red oak to sugar maple or red maple, respectively, were predicted to result in an immediate elevation in leaching due to the slow increase in maple biomass (and associated plant N storage) combined with decreased N storage in

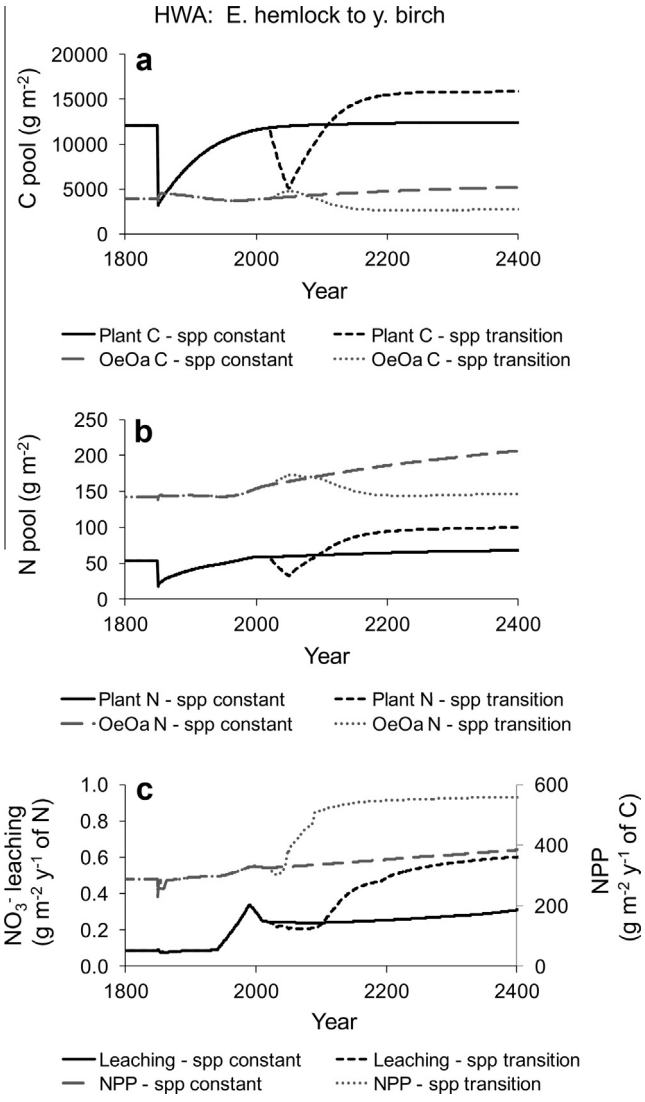

Fig. 7. Comparison of Spe-CN model predictions of (a) C pools in vegetation and OeOa horizons of the forest floor, (b) N pools in vegetation and OeOa horizons of the forest floor, and (c) NPP and NO_3^- leaching between an un-invaded eastern hemlock stand and a stand where yellow birch replaces hemlock due to invasion of HWA. Changes over time are in response to 100% mortality of hemlock in 1850; an increase in N deposition from 0.2 to 1.11 g m^{-2} $year^{-1}$ of N from 1940 to 1990, decreasing to 0.67 g m^{-2} $year^{-1}$ of N by 2010 (Table 1); and a transition from hemlock to yellow birch from 2020 to 2050.

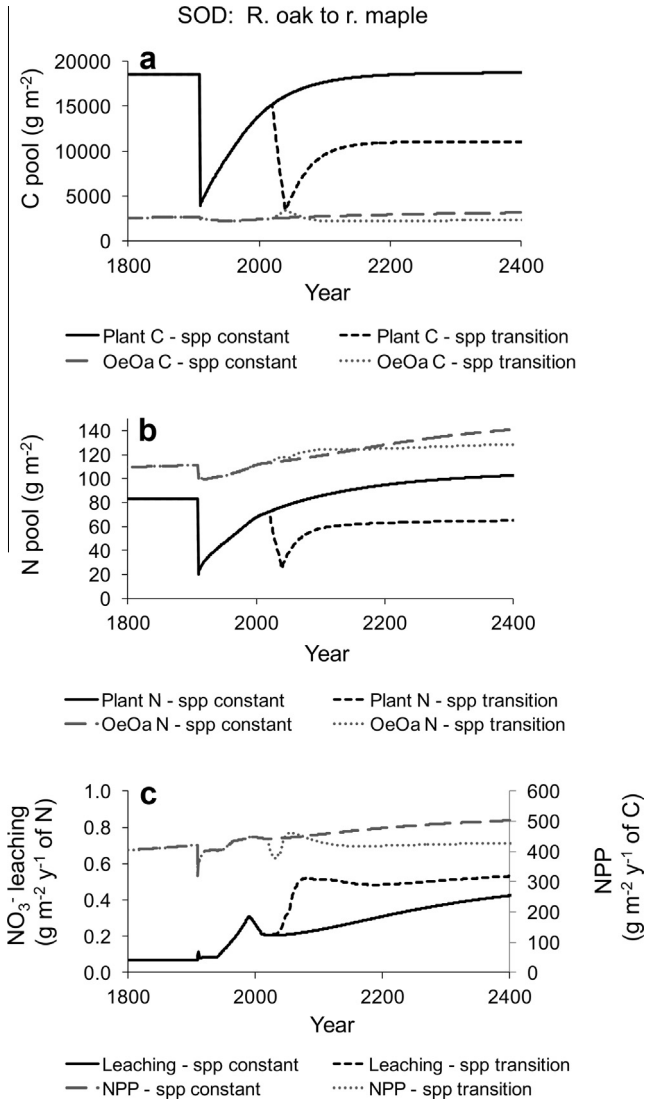

Fig. 8. Comparison of Spe-CN model predictions of (a) C pools in vegetation and OeOa horizons of the forest floor, (b) N pools in vegetation and OeOa horizons of the forest floor, and (c) NPP and NO_3^- leaching between an un-invaded red oak stand and a stand where red maple replaces oak due to invasion of SOD. Changes over time are in response to an 80% harvest in 1910; an increase in N deposition from 0.2 to 1.11 g m^{-2} $year^{-1}$ of N from 1940 to 1990, decreasing to 0.67 g m^{-2} $year^{-1}$ of N by 2010 (Table 1); and a transition from red oak to red maple from 2020 to 2040.

soils and downed wood pools. In contrast, the model predicted that NO_3^- leaching following a transition from hemlock to yellow birch would remain low initially but increase over time with decreasing soil C:N and higher nitrification rates in the new birch stand. The differences in predicted NO_3^- leaching trends among the three invasion scenarios arose from the model's predictions of net N loss from plant, soil, and downed wood pools, which were rapid following BBD or SOD invasion and followed a lag in the case of HWA.

4. Discussion

Insect and disease invasions occurring or anticipated to occur in northeastern U.S. forests are poised to substantially alter forest C and N cycling by causing changes in dominant tree species. Our results suggest that the magnitude and direction of changes in C and N pools and process rates will vary according to interactions between tree species identity and time since invasion, thus generating unique responses for each invasion/stand-response scenario.

4.1. Carbon storage

Early responses to insect or disease invasion of forests have typically included reductions in NPP, particularly due to tree mortality, followed by increased decomposition associated with large additions of organic matter to the forest floor (reviewed in Hicke et al., 2012). Consistent with these patterns and extending them in time, Spe-CN model predictions of net C loss 100 years following the beginning of an invasion (Fig. 6a, Table 2) are supported by field data from plots of comparable age. For example, similar to the simulated beech-maple transition, Finzi et al. (1998) found significantly lower forest floor C underlying a sugar maple canopy relative to a beech canopy, and Lovett et al. (2004, 2013a) observed a non-significant trend toward lower forest floor C underlying sugar maple than beech. Forest floor C:N was also lower in plots dominated by sugar maple vs. beech in the Catskills and in Connecticut (Finzi et al., 1998; Lovett et al., 2004). Along a gradient of stands with increasing BBD impact and consequently greater abundance

of sugar maple, Lovett et al. (2010) found increased litter decomposition and a lower soil C:N ratio, which also corresponds to Spe-CN model predictions of smaller forest floor C and N pools and a lower C:N ratio in a young sugar maple stand transitioning from beech. Simulated species replacements due to HWA and SOD corresponded similarly to field data: Catskills plots dominated by yellow birch had lower forest floor C and C:N ratios relative to hemlock plots (Lovett et al., 2013a, 2004), and Connecticut plots dominated by red maple had lower forest floor C and C:N ratios than did red oak plots (Finzi et al., 1998). Model predictions were driven largely by lower lignin concentrations associated with faster litter decomposition rates for the replacing species (sugar maple, yellow birch, and red maple) than for the initial species (beech, hemlock, and red oak, respectively).

Few field data are available regarding long-term effects of species change on forest C storage or loss. However, the minimal simulated effect of a transition from hemlock to yellow birch on long-term net C balance matched other recent field and modeling efforts suggesting that net effects of HWA on regional C fluxes will be small as rapid growth of replacing species compensates for C losses (Albani et al., 2010; Raymer et al., 2013). The increasing divergence in Spe-CN model predictions among invasion scenarios over time also agrees with findings from a recent review, indicating that long term responses of forest C cycling to invasion may be significant but highly variable due to type of infestation, time since disturbance, magnitude of effect, and growth characteristics of the remaining vegetation (Hicke et al., 2012). While northeastern U.S. forests rarely reach 300 years without disturbance from land use change, management activities, or other factors, extending model simulations over this time period illustrates that response patterns attributable solely to shifts in species composition can change substantially as the forest ages, and these complex species-specific responses will interact over time with the changing regional landscape.

4.2. Nitrogen retention and loss

Several studies have found increased rates of N cycling immediately following insect or pathogen invasion (e.g., Griffin and Turner, 2012; Hobara et al., 2001; Jenkins et al., 1999; Lovett et al., 2010; Orwig et al., 2008), but few have investigated such effects over time given long tree life spans (but see Lovett et al., 2010). In a chronosequence of plots invaded by BBD, Lovett et al. (2010) found more extractable soil NO_3^- and higher NO_3^- in soil solution in plots with greater sugar maple abundance, which is consistent with Spe-CN model predictions of greater NO_3^- leaching from a stand transitioning from beech to sugar maple. Red oak also has been observed to inhibit nitrification in the Catskills, suggesting that nitrification and leaching could increase as oak declined (Lovett et al., 2004); this also corresponds to model simulations of greater leaching following a transition from red oak to red maple due to SOD. For the HWA-induced transition from hemlock to yellow birch, the predicted NO_3^- leaching increase is consistent with distinct N-cycling profiles observed in stands dominated by yellow birch (with high foliar and litter N) relative to hemlock (low litter N and low N mineralization and nitrification rates; Lovett et al., 2004). Model predictions suggested a 100-year time frame for reductions in soil C:N underlying the new birch stand to stimulate nitrification and associated N loss from soils. Predictions of higher NO_3^- leaching following a hemlock-birch transition also agree with the greater inorganic N availability and nitrification rates found in stands with higher hemlock mortality in a chronosequence in southern New England, although this sequence represented a shorter time scale (Jenkins et al., 1999), and with high NO_3^- leaching in stands with experimentally-induced hemlock mortality (Yorks et al., 2003). As for C, Spe-CN model predictions of N dynamics varied depending on the interaction between species and time since invasion.

4.3. Implications

Overall, modeling scenarios concurred with field studies concluding that insect and pathogen invasions will influence long-term forest nutrient cycling largely due to changing tree species composition (Cobb, 2010; Cobb et al., 2013; Jenkins et al., 1999; Lovett et al., 2010; Orwig et al., 2008). Using modeling approaches to extend field results to a longer time scale emphasizes that interactions between tree species change and forest age have potential to generate considerable variability in the role of northeastern U.S. forests as net sources or sinks for C or N over time. Predicted variability in the magnitude, direction, and timing of invasion effects on C and N cycling has several key implications. First, the predicted range in net C balance among simulations of BBD, HWA, and SOD was large, from a maximum net C loss of 9.7 kg m^{-2} in the transition from red oak to red maple to a maximum increase in C storage of 2.8 kg m^{-2} in the transition from beech to sugar maple. This suggests that predictions of future C storage in northeastern U.S. forests are unlikely to be accurate unless they account for changes in species composition.

Second, across the three invasion scenarios, the Spe-CN model predicted a net loss of C due to species replacement for a minimum of 145 years following invasion; the magnitude of predicted C loss from invaded forests during this time period varied with the identity of the declining and compensating species. These results suggest that forested landscapes subject to these three invaders, and maintained largely as second-growth forest (i.e., forest age < 145 - years), could become net sources of CO_2 to the atmosphere. Under current forest management practices, a majority of forests in the northeastern U.S. are actively managed (Canham et al., 2013) and could fall into this category if also subject to invasion. Regionally and over time, the magnitude of CO_2 release would depend on the interaction between the extent of invasion, the distribution of the declining and compensating species, and the age of the recovering forest.

Third, the model predicted that changes in tree species composition due to invasion can unlock large pools of N stored in the forest floor, causing elevated leaching. The timing of the leaching increase depends on the species change scenario, however, and may lag behind the invasion due to legacy effects in the forest floor. Together, these model predictions suggest that achieving goals to increase C storage or reduce NO_3^- leaching in northeastern U.S. forests will require accounting for the variable effects of changing tree species composition on patterns of C and N retention and loss.

4.4. Challenges and opportunities

4.4.1. Challenges

Understanding of species-specific effects on forest C and N cycling is incomplete in several areas that were accordingly difficult to model, particularly in relation to N dynamics (reviewed in Hobbie, 2015). The most notable modeling challenges were in the simulation of belowground processes, which are poorly constrained yet strongly influence the movement of C and N. For example, studies show that higher N concentrations in foliar litter can slow litter decomposition (Berg, 2014; Cornwell and Weedon, 2014); however, higher foliar litter N increases the fraction of slowly cycling litter in some cases but not others, and the relationship is therefore difficult to simulate in ecosystem models (Hobbie, 2015), although it has been incorporated in some cases (Tonitto et al., 2014; Whittinghill et al., 2012). Also constraining modeling efforts, N dynamics associated with decomposing roots are known to differ from those of foliar litter (Hobbie et al., 2010), but these

root-specific differences in N immobilization and release require further study (Hobbie, 2015). Finally, evidence exists for rapid soil immobilization of NO_3^- and NH_4^+ that varies with species composition and forest age and may be partially abiotic (Berntson and Aber, 2000; Colman et al., 2008; Dail et al., 2001; Fitzhugh et al., 2003; Lewis et al., 2014), but the capacity and reversibility of this fast soil sink are unknown. Many studies have examined movement of inorganic N into soils and vegetation using a 15-N tracer (Nadelhoffer et al., 1999; e.g., Nadelhoffer et al., 1995; Templer et al., 2005); however, further study is needed to generalize NO_3^- and NH_4^+ partitioning among soil pools and to simulate and parameterize N immobilization processes effectively in a modeling context.

As for the processes governing decomposition and N dynamics, further study belowground is needed to improve estimation of several species-specific parameter values. For example, the Spe-CN model employs a mycorrhizal N pool to simulate greater access by EM than AM species to N from the organic (humus) pool; EM fungi make more N available to plants, in line with an organic vs. inorganic mycorrhizal nutrient economy (Langley and Hungate, 2003; Phillips et al., 2013). Within this general framework, we have little data to constrain the species-specific fractions of N following this pathway. Non-foliar plant tissues contribute significantly to decomposition dynamics (Freschet et al., 2013; Hobbie, 2015), but there are many fewer studies of decomposition of roots and stems than foliage. Data are also insufficient regarding SOM decomposition rates and transfer of material among SOM (e.g., active and passive) pools, particularly in relation to species composition, which may affect decomposition of SOM pools differently from surface litter (Hobbie, 2015; Prescott, 2010; Vesterdal et al., 2012). Finally, we simulated N mineralization from soil pools as a function of C mineralization, modified by the ratio of net to gross N mineralization, yet few data are available to constrain this ratio. Further refinement of all of these parameters as more data become available should improve predictions of species-specific effects on C and N cycling.

The Spe-CN model provides a tool for synthesizing what has been learned from decades of empirical, species-specific research in the forests of the northeastern U.S. Because our understanding of species-specific effects on nutrient cycling remains incomplete, particularly belowground, individual values predicted by the model have uncertainty associated with them. The large pool of species-specific research available to inform key areas of model development, however, makes our confidence high overall in the broad species-specific patterns that the model predicts.

4.4.2. Opportunities

We developed the Spe-CN model to quantify species-specific contributions to differences in C and N cycling across the landscape, which are distinct from effects of site-level factors (e.g., soil texture, water dynamics, detailed land use history) that also influence forest nutrient dynamics. However, forest change due to invasive pests over the next 50–100 years will unfold in concert with changes in other environmental factors, such as atmospheric CO_2 and climate, that also influence C and N cycling directly. In this paper we have isolated and focused on effects of species change due to pest invasions; future work on the model will allow us to simulate climate change and pest invasions together. To do this we will need to add a hydrologic submodel to simulate water availability to plants and decomposers, and a routine that simulates direct effects of temperature, water, and CO_2 on primary production. These alterations to the model are under development.

Future modeling could also explore ways of driving species change other than the user-set scenarios described here—for instance, species change scenarios could be the output of suitable-habitat models such as DISTRIB (Iverson et al., 2008a,b), or Spe-CN could interface with a community dynamics model such as Sortie (Pacala et al., 1996). To refine predictions of invasive insect and disease impacts, future efforts could incorporate physiological effects of invaders on specific plant tissues (Dietze and Matthes, 2014; Hicke et al., 2012). Finally, future simulations could investigate the effects on C storage and NO_3^- leaching of different types of forest management response to invasion; evaluation of different types of species change combined with alternative management strategies will generate multiple scenarios with complex interactions. These further refinements and applications of the Spe-CN model would enable questions regarding interactions between species transitions (due to invasive insects and pathogens, climate change, or other disturbances) and the direct effects of climate change, N deposition, management activities, and other impacts to northeastern U.S. forests.

5. Conclusions

Modeling simulations demonstrated that changes in tree species composition associated with invasive insects and diseases have potential to alter forest C and N dynamics considerably over short and longer time periods. Tree species replacements may change the distribution of C and N between plant and soil pools, resulting in a large range in potential net changes in C and N storage among invasion types. Responses to tree species change will depend on the identities of the declining and compensating species and their associated plant traits, which influence rates of production, litterfall, decomposition, and therefore C and N retention and loss. These responses may also change over time, with different patterns evident in younger and older forests, again depending on the identity of the species involved. Active forest management in the northeastern U.S., which maintains large areas of younger forest, may interact with invasion effects to reduce the forest's ability to store C. Finally, changes in tree species composition due to invasion can release N stored in the forest floor and cause elevated leaching, with timing dependent on tree species identity. This work shows that predictions of C and N dynamics in the future will need to account for tree species change over short and long time scales in order to generate meaningful estimates of C and N storage and loss in northeastern U.S. forests.

Acknowledgments

We would like to thank numerous researchers in northeastern U.S. forests whose work has provided data needed to develop, parameterize, and test the Spe-CN model. We also thank two anonymous reviewers for helpful comments on the manuscript. This research was funded by the U.S. National Science Foundation (award #DEB 0948780), the New York State Energy Research and Development Authority (agreement #40508), and the USDA Agriculture and Food Research Initiative Program (award #2015-67019-23496).

Appendix A. Detailed model description

Our primary objective in developing the Spe-CN model was to simulate differences in forest C and N cycling attributable to changes in tree species composition. We used algorithms developed from field-based empirical relationships wherever possible, and parameterized the model using data from the northeastern U.S (Tables A.1 and A.2). We also adapted relevant approaches from existing ecosystem models such as PnET-CN (Aber and Federer, 1992; Aber et al., 1997) and CENTURY (Parton et al., 1987, 1988) where they could be tailored to a species-specific context. Key procedures in the model govern production of new biomass, using

available N to support production; production of litter; decomposition in forest floor, mineral soil, and CWD pools; and leaching of NO_3^- not taken up by vegetation or soil (Fig. 1).

A.1. Production, allocation, and N uptake

In the Spe-CN model, NPP is a function of foliar N, based on empirical relationships between canopy N and aboveground NPP (ANPP) for angiosperm and gymnosperm tree species (Smith et al., 2002). The generalized version of the relationship is as follows:

$$\text{NominalNPP}_i = 0.5 \times \text{ProdFraction}_i \times \text{Bmult} \times (1/(1-\text{RootProdFrac}) \times (\text{ANPPslope} \times \text{NewFolNcon}_i + \text{ANPPint})) \quad (A.1)$$

where NominalNPP_i ($g\ m^{-2}\ year^{-1}$ of C) is the yearly estimate of total NPP for a given species (i) in the absence of N limitation. ProdFraction_i is the specified fraction of total production for that species, analogous to the fraction of canopy space occupied by the species. The parameter Bmult is a function of total wood C, reducing ANPP if wood C is low following a disturbance, such that stands with low biomass do not achieve full NPP. RootProdFrac is the fine root fraction of total NPP for angiosperms (RootProdFracAngio) or gymnosperms (RootProdFracGymno), and the ANPPslope and ANPPint are the slope and intercept of the linear relationship between foliar N (%) and ANPP ($g\ m^{-2}\ year^{-1}$ of dry mass) for angiosperms or gymnosperms (see Table A.1 for values specific to angiosperm or gymnosperm species; Smith et al., 2002). The multiplier 0.5 converts the estimate of ANPP from g of dry matter to g of C, assuming that plant biomass is 50% C. NewFolNcon_i (%) represents the foliar N concentration for a given species (i), adjusted to reflect a species' N status in the stand within a species-defined range:

$$\text{NewFolNcon}_i = \text{MinFolNCon}_i \times \text{Nratio}_i \quad (A.2)$$

where MinFolNCon_i (%) is the minimum foliar N concentration for a given species (Tables A.1 and A.2). The parameter Nratio_i (adapted from Aber et al., 1997) is a function of current plant N concentration (PlantNconScale_i, scaled between 0 and MaxPlantNCon_i) relative to the maximum possible plant N concentration at the current plant C (MaxPlantNCon_i), adjusted by a species' potential range in foliar N concentration (FolNConRange_i):

$$\text{Nratio}_i = 1 + (\text{PlantNconScale}_i/\text{MaxPlantNCon}_i) \times \text{FolNConRange}_i \quad (A.3)$$

NRatio_i thus varies between 1 and 1 + FolNConRange. Nratio_i is used to calculate the N concentrations of all plant tissues (foliage, roots, fine wood, and coarse wood) within a potential range for each species and tissue type, to reflect the level of N sufficiency within the plant (Aber et al., 1997). Allocation of ANPP to wood vs. foliage for angiosperms is also a function of foliar N, such that allocation to foliage decreases linearly as foliar N increases (Table A.1; Smith et al., 2002).

Plant N uptake to support NPP is determined by growth and tissue N concentration. Nitrogen taken up from soil inorganic NO_3^- and NH_4^+ pools is stored as "mobile" N within the coarse and fine wood tissues and used to support production (e.g., Millard and Grelet, 2010). Inorganic N from each soil pool is allocated among tree species based on their fraction of total stand production. Mycorrhizal N (MycoN) is allocated among species based on mycorrhizal status (EM species receive a greater fraction of MycoN than do AM species (Langley and Hungate, 2003)) and relative N demand for each species in the stand. If insufficient N is available from inorganic soil N pools, stored mobile N in the plant, and the mycorrhizal N pool to support NPP, then actual NPP is scaled back accordingly from the nominal value.

A.2. Litter production

Turnover of foliage, roots, fine wood, and fragmented coarse wood move plant material into the litter and subsequently the humus pool, which together make up the forest floor, while unfragmented CWD moves into a separate pool.

Foliar litter enters the litter pool annually at the end of the growing season, and foliar turnover differs for angiosperm vs. gymnosperm species (Tables A.1 and A.2). The fraction of N resorbed from foliage before litterfall is species-specific, and resorbed N moves into a bud N pool that combines with mobile N to support the following year's NPP. Non-foliar litter types enter the litter pool monthly. Root turnover is a function of available soil N (Aber et al., 1985); fine wood turnover is a constant value (Fahey et al., 2005); and a fraction of CWD fragments and enters the litter pool (Table A.1). Root turnover occurs according to the following relationship:

$$\text{RootTurnoverN} = \text{RootTurnInt} + \text{RootTurnA} \times (\text{TotNAvailYear} \times 10) + \text{RootTurnB} \times (\text{TotNAvailYear} \times 10)^2 \quad (A.4)$$

where RootTurnoverN is the annual root turnover rate ($year^{-1}$), and TotNAvailYear is total annual available soil N ($g\ m^{-2}$ of N, multiplied by 10 to convert to $kg\ ha^{-1}$ of N). RootTurnInt is the intercept in the relationship between N availability and root turnover, and RootTurnA and RootTurnB are the coefficients of the relationship (Aber et al., 1985; Table A.1). Monthly root turnover is calculated from the annual estimate and assumed to be the same throughout the year.

Coarse wood turnover is a function of the maximum wood biomass attainable in pure stands of each species (Tables A.1 and A.2), such that coarse wood biomass cannot exceed a maximum species-specific value. Before moving into decomposing litter and CWD pools, coarse and fine wood initially enter newly dead coarse and fine wood pools with distinct turnover rates, which represent standing dead or other wood not yet in contact with the forest floor.

A.3. Litter decomposition

Litter entering the forest floor is divided into lignin-associated (LA; lignin plus cellulose) and non-lignin-associated (NLA) pools for each species (i), based on relationships derived from the Long-Term Intersite Decomposition Experiment (LIDET; Parton et al., 2007) and applied in the PnET-SOM model (Tonitto et al., 2014). Similar relationships are also applied in the CENTURY model (Parton et al., 1987, 1988). The percentage of litter mass entering the species-specific NLA vs. LA pools follows these relationships:

$$\text{NLA}_i = 90 - 1.4 \times \text{Lignin}_i/(\text{N}_i \times E_N) \quad (A.5)$$

$$\text{LA}_i = 100 - \text{NLA}_i \quad (A.6)$$

where Lignin_i and N_i are the concentrations (%) of lignin and N in litter for a given species. The parameter E_N is a multiplier representing the influence of vegetation type on effective litter N concentration at a site. For an evergreen stand, $E_N = 1$. For a deciduous stand:

$$\begin{aligned} &\text{if } \text{LC}_i \le 0.2 \text{ then } E_N = 5; \\ &\text{if } 0.2 < \text{LC}_i \le 0.4 \text{ then } E_N = 2 + (0.4 - \text{LC}_i) \times 15; \\ &\text{if } \text{LC}_i > 0.4 \text{ then } E_N = 2 \end{aligned} \quad (A.7)$$

where LC_i is the ratio of lignin to cellulose for a given species (Parton et al., 2007).

Table A.1
Summary of parameters used in the Spe-CN model. Species-specific parameters are indicated with a value of * and provided by species in Table A.2. Units are provided within the parameter descriptions, except where parameters are dimensionless.

Parameter	Description	Value	References
Production			
AngioANPPslope	Slope of relationship between foliar N (%) and ANPP (g m^{-2} $year^{-1}$ of dry mass) for angiosperms	361.86	Smith et al. (2002)
AngioANPPint	Intercept of relationship between foliar N (%) and ANPP (g m^{-2} $year^{-1}$ of dry mass) for angiosperms	−122.17	Smith et al. (2002)
GymnoANPPslope	Slope of relationship between foliar N (%) and ANPP (g m^{-2} $year^{-1}$ of dry mass) for gymnosperms	486.15	Smith et al. (2002)
GymnoANPPint	Intercept of relationship between foliar N (%) and ANPP (g m^{-2} $year^{-1}$ of dry mass) for gymnosperms	−246.46	Smith et al. (2002)
MinFolNCon	Minimum foliar N (%) = 10th percentile (P10) in NERC foliar chemistry database	*	NERC (2010)
FolNConRange	Fractional range in foliar N (%) from 10th to 90th percentile ((P90–P10)/P10)	*	NERC (2010)
MinRootNCon	Minimum root N (%) = 80% of mean value	*	Aber et al. (1990), Fahey et al. (1988), McClaugherty et al. (1982, 1984), Templer et al. (2005)
MinFineWoodNcon	Minimum fine wood N (%) = 80% of mean value	*	Pare et al. (2013)
MinCoarseWood Ncon	Minimum coarse wood N (%) = 80% of mean value	*	Fahey et al. (1988), Templer et al. (2005)
Allocation and biomass			
FolAllocAngioA	Slope of relationship between foliar N (%) and foliar allocation fraction (of ANPP) for angiosperms	−0.0864	Smith et al. (2002)
FolAllocAngioB	Intercept of relationship between foliar N (%) and foliar allocation fraction (of ANPP) for angiosperms	0.5266	Smith et al. (2002)
RootProdFracAngio	Fine root fraction of total NPP for angiosperms	0.31	Nadelhoffer and Raich (1992)
FolAllocGymnoA	Foliar fraction of ANPP for gymnosperms	0.37	Smith et al. (2002)
RootProdFracGym	Fine root fraction of total NPP for gymnosperms	0.23	Nadelhoffer and Raich (1992)
CWDFrac	Coarse woody debris (CWD) fraction of total wood litter	0.7	Fahey et al. (2005)
RootCWDFrac	Coarse root fraction of total CWD	0.25	Fahey et al. (2005)
NomMaxWoodC	Maximum wood C (g m^{-2}) (mean of highest 3 available values for each species)	*	Baskerville (1965), Campbell and Gower (2000), Goodale and Aber (2001), Lovett et al. (2013a), Magill et al. (2004), Park et al. (2008), Pregitzer et al. (2008), Sprugel (1984), USFS (2013)
Litterfall and litter decomposition			
FolTurnover	Foliar turnover ($year^{-1}$)	*	Aber et al. (1995)
RootTurnA	Coefficient in relationship between N availability (g m^{-2}) and root turnover ($year^{-1}$)	−0.0191	Aber et al. (1985)
RootTurnB	Coefficient in relationship between N availability (g m^{-2}) and root turnover ($year^{-1}$)	0.000211	Aber et al. (1985)
RootTurnInt	Intercept in relationship between N availability (g m^{-2}) and root turnover ($year^{-1}$)	0.789	Aber et al. (1985)
FineWoodTurnover	Fine wood turnover ($year^{-1}$)	0.025	Fahey et al. (2005)
NewDeadFine WoodTurn	Turnover of newly dead fine wood to fine litterfall ($year^{-1}$)	0.5	Estimated value
NewDeadCoarse WoodTurn	Turnover of newly dead coarse wood to CWD ($year^{-1}$)	0.1	Estimated value
kFragCWD	Physical fragmentation rate for CWD ($year^{-1}$)	0.01	Estimated value
CoarseWoodk	Decomposition constant for CWD ($year^{-1}$)	*	Fahey et al. (1988), Foster and Lang (1982), Lambert et al. (1980), Macmillan (1988), Smith et al. (2007), Tyrrell and Crow (1994)
NGRatioCWD	Ratio of net to gross N mineralization in CWD	0.3	Estimated value
FolLigCon	Mean foliar litter lignin concentration (%)	*	Aber et al. (1990), Downs et al. (1996), Hobbie et al. (2006), Lovett et al. (2004), Magill and Aber (1998), Melillo et al. (1982), Piatek et al. (2009), Pouyat and Carreiro (2003)
RootLigCon	Mean root lignin concentration (%)	*	Aber et al. (1990), Fahey et al. (1988), McClaugherty et al. (1982, 1984)
FineWoodLigCon	Mean fine wood lignin concentration (%)	*	Alban and Pastor (1993), Macmillan (1988)
CoarseWoodLigCon	Mean coarse wood lignin concentration (%)	*	Alban and Pastor (1993), Macmillan (1988)
FolLigCell	Foliar lignin:cellulose ratio	*	NERC (2010)
Lignink	Decomposition constant for lignin component of litter ($year^{-1}$)	0.14	Parton et al. (2007)
Cellulosek	Decomposition constant for cellulose component of litter ($year^{-1}$)	0.25	Parton et al. (2007)
NLAk	Decomposition constant for labile (NLA: non-lignin-associated) component of litter ($year^{-1}$)	2.82	Parton et al. (2007)
LACN	C:N ratio of lignin-associated material (LA: lignin + cellulose) in litter	150	Parton et al. (1987)
CDI	Climate Decomposition Index. Value is for Coweeta Hydrological Laboratory and sets a southern limit for application of the Spe-CN model	0.41	Parton et al. (2007)
FolNML	Slope of the relationship between litter N (%) and mass loss (%) for foliar litter	*	Aber et al. (1990), Demers et al. (2007), Gosz et al. (1973), Lovett et al. (2015, 2010), Magill and Aber (1998), Melillo et al. (1982), Piatek et al. (2009), Pouyat and Carreiro (2003)

Table A.1 (*continued*)

Parameter	Description	Value	References
RootNML	Slope of the relationship between litter N (%) and mass loss (%) for fine roots	*	Aber et al. (1990), McClaugherty et al. (1984)
FineWoodNML	Slope of the relationship between litter N (%) and mass loss (%) for fine wood	*	Foster and Lang (1982)
CoarseWoodNML	Slope of the relationship between litter N (%) and mass loss (%) for coarse wood	*	Foster and Lang (1982)
Resorp	Ratio between mean foliar litter N (%) and foliar N (%)	*	Aber et al. (1990), Boerner (1984), Boerner and Rebbeck (1995), Cobb (2010), Downs et al. (1996), Gartner and Cardon (2006), Gosz et al. (1973), Gower and Son (1992), Hobbie (2005), Kaczmarek et al. (1998), Lovett et al. (2015, 2010), Magill and Aber (1998), Melillo et al. (1982), NERC (2010), Norby et al. (2000), Piatek et al. (2009), Polyakova and Billor (2007), Pouyat and Carreiro (2003), Pregitzer et al. (1992), Rustad (1994), Templer et al. (2005), Zak et al. (1986)
CohortPctNMax	Asymptote of litter N (%) as a function of mass loss (%) after 2 years of decomposition	2.5	Aber et al. (1990), Bockheim et al. (1991), Cobb (2010), Demers et al. (2007), Gosz et al. (1973), Lovett et al. (2015, 2010), Magill and Aber (1998), Melillo et al. (1982), Parsons et al. (2008), Piatek et al. (2009), Pouyat and Carreiro (2003), Rustad (1994), Strukelj et al. (2012)
Humus and mineral soil			
HumusSpk	Decomposition constant for humus ($year^{-1}$)	*	Estimated based on Parton et al. (1988), Olsson et al. (2012), Tonitto et al. (2014)
kASOM	Decomposition constant for active soil organic matter (SOM) ($year^{-1}$)	0.007	Tonitto et al. (2014)
kPSOM	Decomposition constant for passive SOM ($year^{-1}$)	0.001	Tonitto et al. (2014)
HSOMTran	Fraction of humus transferred to SOM at end of growing season	0.005	Tonitto et al. (2014)
PSOMFrac	Passive fraction of material transferred from humus to SOM	0.7	Estimated based on data in McFarlane et al. (2013), Rodriguez et al. (2014)
HumusNGR	Ratio of net to gross N mineralization in humus	*	Estimated to reproduce range of soil C:N under Catskills tree species
SOMNGR	Ratio of net to gross N mineralization in SOM	0.9	Estimated to reproduce relationship between C:N of humus and C:N of active SOM in the Catskills
MycoNFrac	Fraction of N mineralized from humus that moves into the MycoN pool, and fraction of MycoN allocated to each species	*	Estimated value
MiningMax	Limit on enhancement of decomposition during N limitation	0.3	Estimated value
Nitrification and leaching			
NitfracFFslope	Slope of relationship between C:N ratio and nitrification fraction of N mineralization for the forest floor	−0.0732	Lovett et al. (2004)
NitfracFFint	Intercept of relationship between C:N ratio and nitrification fraction of N mineralization for the forest floor	1.8924	Lovett et al. (2004)
NitfracSOMslope	Slope of relationship between C:N ratio and nitrification fraction of N mineralization for SOM	−0.0482	Lovett et al. (2004)
NitfracSOMint	Intercept of relationship between C:N ratio and nitrification fraction of N mineralization for SOM	1.4142	Lovett et al. (2004)
MinNitFraction	Minimum value for the fraction of mineralized N that nitrifies	0.01	Estimated based on data in Lovett et al. (2004)
NH4nitFraction	Fraction of litter NH_4^+ that nitrifies	0.05	Estimated value
N deposition			
NDepNO3frac	NO_3^- fraction of total (NO_3^- + NH_4^+) N deposition	0.75	Ollinger et al. (1995, 1993)
NdepNO3SoilFrac	Fraction of NO_3^-–N from N deposition that moves into soil N pools	0.3	Estimated based on data in Fitzhugh et al. (2003)
NdepNO3LitterFrac	Fraction of the soil component of NO_3^-–N deposition that moves into litter vs. humus	0.5	Estimated based on data in Nadelhoffer et al. (1999)
NdepNH4SoilFrac	Fraction of NH_4^+–N from N deposition that moves into soil N pools	0.6	Estimated based on data in Fitzhugh et al. (2003), Templer et al. (2005)
NdepNH4LitterFrac	Fraction of the soil component of NH_4^+–N deposition that moves into litter vs. humus	0.5	Estimated based on data in Nadelhoffer et al. (1999)

Decomposition is calculated monthly for each species (i) and each of three litter cohorts (j), as follows:

For the LA pool:

$$\text{Closs}_{ij} = \text{LAC}_{ij} \times \text{LAk} \times (\text{fraction of year}) \times \text{TMultK} \times \text{CDI} \times \text{MiningMult} \quad (A.8)$$

And for the NLA pool:

$$\text{Closs}_{ij} = \text{NLAC}_{ij} \times \text{NLAk} \times (\text{fraction of year}) \times \text{TMultK} \times \text{CDI} \times \text{MiningMult} \quad (A.9)$$

where Closs_{ij} is the amount of C ($g\ m^{-2}$) respired in a given month for a particular species and litter cohort; NLAC_{ij} and LAC_{ij} are the litter NLA and LA C pools ($g\ m^{-2}$) for a given species and cohort; and NLAk and LAk are the yearly decomposition constants ($year^{-1}$) for the NLA and LA pools. The fraction of the year is determined from the number of days in a given month. The parameter TMultK is an adjustment for decomposition rate based on monthly mean temperature, developed for PnET (Aber et al., 1997). Because the current version of the model does not simulate water movement, monthly precipitation and soil moisture do not yet influence decomposition.

The modifier CDI is a Climate Decomposition Index for the Coweeta Hydrological Laboratory (Parton et al., 2007), which sets a southern limit for the model's applicable range. The multiplier MiningMult enhances decomposition when the vegetation is N-limited.

For the decay constant for NLA material, NLAk, we used the value calculated for the labile component of litter in the LIDET experiment (Parton et al., 2007). The decay constant for LA material, LAk, represents a weighted average (by litter mass) of the decay constants for lignin and cellulose, given that the percentage of cellulose in litter is 100 – NLA_i – $Lignin_i$ (Parton et al., 2007).

The multiplier MiningMult is calculated as follows:

$$\text{MiningMult} = 1 + (1 - \text{NratioSite})^{1/2} \times \text{MiningMax} \quad \text{(A.10)}$$

where the parameter MiningMax represents the maximum extent to which decomposition can be enhanced, such that MiningMult varies nonlinearly between 1 and (1 + MiningMax). NratioSite represents the extent of N limitation across tree species in the stand and falls between 0 and 1; N limitation is high and decomposition is therefore enhanced when NratioSite is low. NratioSite is calculated from the scaled ratio of current plant N concentration to the maximum possible N concentration for each species' current biomass, weighted by total N in biomass for each species. This algorithm allows plants to accelerate the decomposition of soil organic matter when N is limiting, for instance by increased allocation to mycorrhizae or by releasing C compounds to "prime" microbial decomposition (Phillips et al., 2011).

Nitrogen mineralization and N immobilization in each of the three decomposing litter cohorts are described by the slope of the relationship between litter N concentration (%) and mass loss (%) (N mass loss or NML; e.g., Aber et al., 1990), a species-specific value obtained from litter bag experiments (Tables A.1 and A.2). The NML relationship describes a strong, linear increase in litter N concentration with increasing mass loss during the first phase of the decomposition process (Aber and Melillo, 1982; Aber et al., 1990). We used the NML slope to calculate N concentration in the decomposing litter cohorts on a monthly basis:

$$\text{PercentN}_{ij} = \text{InitialNCon}_{ij} + \text{NML}_{ij} \times \text{PercentMassLoss}_{ij} \quad \text{(A.11)}$$

where PercentN_{ij} (%) is the new N concentration for a species-specific litter cohort; InitialNCon_{ij} (%) is the initial litter N concentration for a given species in the cohort; NML_{ij} (dimensionless) represents the NML slope for a given species; and $\text{PercentMassLoss}_{ij}$ (%) is the total mass loss (across NLA and LA fractions) for this species and cohort. The difference in cohort N between the prior and current month (where cohort N (g m^{-2}) is calculated from N concentration (%) and cohort mass (g m^{-2} of dry matter, with dry matter assumed to be 50% C)) is then used to calculate the amount of N mineralized or immobilized monthly from each cohort, by species. The three litter cohorts (representing three growing seasons) encompass the period during which N immobilization may occur in the litter, as determined from the NML relationship. Microbial N immobilization is limited to NH_4^+–N from atmospheric N deposition plus NH_4^+–N mineralized from the humus, active SOM, and passive SOM pools in the current month. At the end of each growing season, C and N in each litter cohort are transferred to the next cohort, and C and N in the oldest cohort are transferred to the humus pool.

A.4. Decomposition in other soil and CWD pools

In the humus, active SOM, passive SOM, and CWD pools, C mineralization occurs according to the following generalized equation:

$$\text{CLoss} = \text{TotalC} \times k \times (\text{fraction of year}) \times \text{TMultK} \times \text{MiningMult} \quad \text{(A.12)}$$

where Closs (g m^{-2} of C) represents monthly C loss for a given pool; TotalC is the total amount of C in the pool; k is the yearly decomposition constant for the pool (Tables A.1 and A.2); and TmultK and MiningMult are as described above for litter decomposition. The multiplier TMultK applies in the humus, Active SOM, and CWD pools, which are considered most sensitive to temperature. The parameter MiningMult applies in the humus, Active SOM, and Passive SOM pools; this assumes no enhancement of decomposition due to mining in the CWD pool. In the humus pool, values of k vary for angiosperm vs. gymnosperm species (Olsson et al., 2012; Vesterdal et al., 2012), and humusk represents a weighted average of litter contributions. At the end of the growing season, a fraction of the C and N in the humus pool is transferred to mineral soil (Tonitto et al., 2014) and divided between active SOM and passive SOM, at which point species composition no longer influences

Table A.2
Species-specific parameter estimates for the Spe-CN model. For parameter descriptions and sources, see Table A.1. Parameters without units are dimensionless.

Parameter (units)	American beech	Eastern hemlock	Red maple	Red oak	Sugar maple	Yellow birch
NE US MinFolNCon (%)	1.88	1.00	1.41	1.53	1.58	2.05
Catskills MinFolNCon (%)	2.2	1.21	1.69	2.12	1.79	2.25
WMNF MinFolNCon (%)	1.93	1.05	1.61	2.07	1.62	2.05
NE US FolNConRange	0.39	0.56	0.54	0.62	0.42	0.40
Catskills FolNConRange	0.21	0.38	0.35	0.25	0.30	0.25
WMNF FolNConRange	0.36	0.50	0.43	0.21	0.40	0.37
MinRootNCon (%)	1.33	0.98	1.30	0.98	1.30	1.38
MinFineWoodNcon (%)	0.24	0.23	0.25	0.19	0.26	0.38
MinCoarseWoodNcon (%)	0.19	0.12	0.18	0.20	0.18	0.20
NomMaxWoodC (g m^{-2} of C)	12,796	11,910	11,422	22,446	21,102	16,683
FolTurnover ($year^{-1}$)	1	0.25	1	1	1	1
CoarseWoodk ($year^{-1}$)	0.06	0.025	0.06	0.06	0.06	0.06
FolLigCon (%)	24.9	14.6	15.4	25.3	13	21.8
RootLigCon (%)	26.8	23.8	26.8	26.8	26.8	26.8
FineWoodLigCon (%)	16.2	28.8	16.2	16.2	16.2	16.2
CoarseWoodLigCon (%)	16.2	28.8	16.2	16.2	16.2	16.2
FolLigCell	0.58	0.52	0.62	0.61	0.55	0.57
FolNML	0.0236	0.0145	0.02	0.021	0.023	0.0236
RootNML	0.019	0.02	0.019	0.019	0.019	0.019
FineWoodNML	0.005	0.005	0.005	0.005	0.005	0.005
CoarseWoodNML	0.005	0.005	0.005	0.005	0.005	0.005
Resorp	0.43	0.53	0.41	0.42	0.4	0.43
HumusSpk ($year^{-1}$)	0.045	0.015	0.045	0.045	0.045	0.045
NGRhumus	0.8	0.8	0.7	0.8	0.7	0.8
MycoNFrac	0.75	0.75	0.25	0.75	0.25	0.75

decomposition rates. These parameters are described in further detail in Table A.1.

Nitrogen mineralization in the humus, active SOM, passive SOM, and CWD pools is a function of C mineralization:

$$\text{Nmin} = \text{CLoss} \times \text{TotalN/TotalC} \times \text{NGR} \quad \text{(A.13)}$$

where Nmin (g m^{-2} of N) is N mineralization for a given pool, calculated from C loss modified by the ratio of net to gross N mineralization (NGR) for the pool. The NGR thus defines the fraction of the mineralized N that moves to soil available N pools. For the humus pool, the NGR is lower for soils underlying AM than EM species, based on the assumption that AM species are poorer competitors with heterotrophic soil microbes, thereby resulting in greater soil N retention in AM- than EM-dominated stands. A greater fraction of N mineralized from the humus moves into the MycoN pool when EM species dominate the stand, leading to greater plant N retention in EM- than AM-dominated stands. Together, these algorithms reflect differences in an AM vs. EM nutrient economy (Averill et al., 2014; Langley and Hungate, 2003; Phillips et al., 2013).

In the Spe-CN model, the fraction of mineralized N that nitrifies is a function of soil C:N (Lovett et al., 2004), which is determined from the dynamics of C and N in the forest floor and SOM pools. Nitrification rate is also a function of overall plant demand for N, via the NRatioSite parameter described above; this assumes that plants compete more strongly for NH_4^+ than do nitrifiers, and nitrification is therefore reduced when plant N demand is high (adapted from Aber et al., 1997). A small fraction of the NH_4^+ in the litter also nitrifies each month. Following nitrification, all inorganic NO_3^- is considered available for plant uptake, and any remaining NO_3^- leaches from the system each month. All NH_4^+–N mineralized from soil pools and not immobilized in litter, nitrified, or reserved as mycorrhizal N is also available for direct plant uptake, and any NH_4^+–N not taken up in the current month remains in inorganic soil pools until the following month.

Appendix B. Detailed analysis of model testing

To test the Spe-CN model for application to stands dominated by sugar maple, beech, yellow birch, hemlock, red oak, or red maple, we compared model simulations to independent field data from plots dominated by single species in the Catskill Mountains (Lovett et al., 2002, 2004, 2013a; Templer et al., 2005), the WMNF (Goodale and Aber, 2001; Ollinger et al., 2002), and the GMF (Finzi et al., 1998; Table 1). We used versions of Spe-CN parameterized with mean monthly temperature, N deposition regime, minimum foliar N concentration, and foliar N range for each sub-region to simulate C and N pools and process rates for second-growth (90 years post-disturbance, the average age of field plots) and old-growth stands (simulated at 300 years) dominated by each species (Figs. 2, 3 and B.1). We then plotted the field data and the range in Spe-CN modeled values for each output variable across the test areas, by species, such that the Spe-CN values reflected the range of temperature, N deposition, and stand ages represented by the field data.

As discussed in Section 2.3, the ranges in Spe-CN modeled values generally corresponded well with available field data from the three test areas (Figs. 2, 3 and B.1). Site-level exceptions appeared to derive from unusual site characteristics or land use history. For example, while simulated plant and soil C and N pools generally fell within two standard errors of mean field data estimates, exceptions included red oak and yellow birch plots from the Catskills. For red oak, Spe-CN overestimated C, N, and C:N for the OeOa horizons in the forest floor, and for yellow birch, Spe-CN underestimated these variables (Fig. 2a–c). In these Catskills yellow birch stands, the forest floor was underlain by rock substrate, which limited development of mineral soil and resulted in a thick organic horizon that the model was unable to simulate. We estimate that the red oak stands burned 60–90 years before the plots were sampled, which may have reduced the thickness of the forest floor, although we would expect forest floor recovery over this length of time. For red maple and hemlock, field measurements of OeOa C:N were highly variable across sites and regions (Fig. 2c). Spe-CN simulations of OeOa C:N thus fell within a narrower range than the field data, perhaps due to variability in factors such as soil substrate, landscape position, or landscape history across sites dominated by these species. The broad range in field C:N could also be due to other species present in the limited number of available field plots, as composition of additional species was variable in plots dominated by red maple and hemlock.

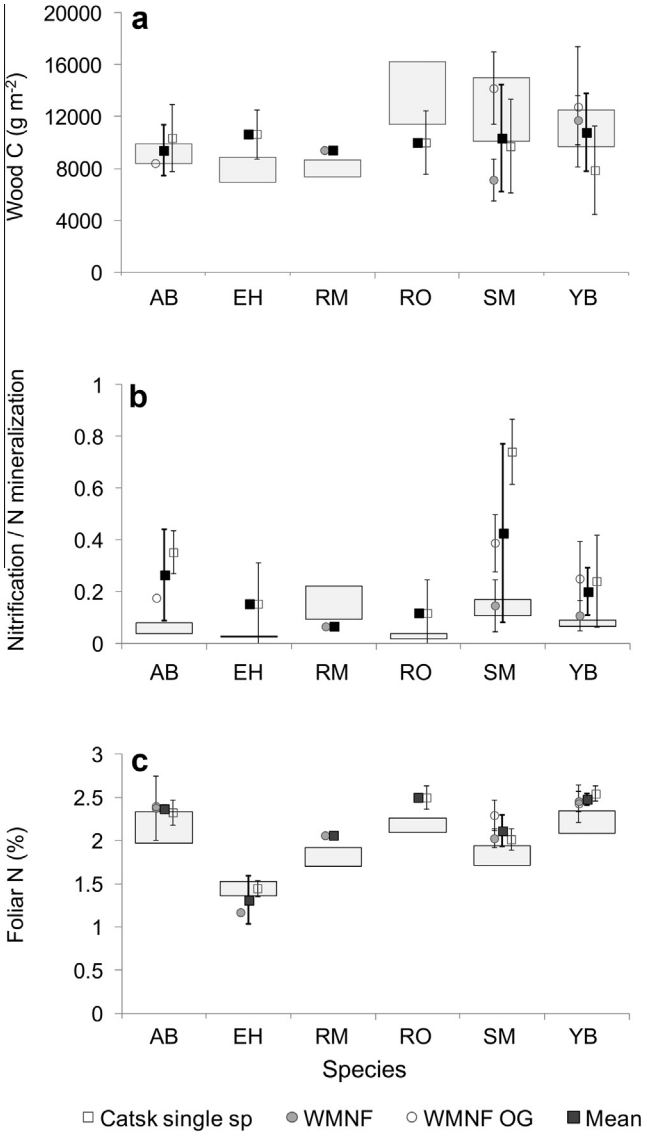

Fig. B.1. Comparison of Spe-CN model simulations to field data from plots dominated by single species for (a) wood C, (b) the ratio of nitrification to N mineralization for the OeOa horizons in the forest floor, and (c) foliar N. On each plot, the bars provide the range of Spe-CN modeled values across N deposition, temperature, and stand ages associated with field data from the Catskills, WMNF, and/or GMF. Points give the mean value ±2 standard errors for field data within each sub-region and across the three sub-regions (labeled as "Mean"). Field data indicated as "OG" are from old-growth forest, simulated at 300 years post-disturbance; other field data are from second-growth forest, simulated at 90 years. AB = American beech; EH = eastern hemlock; RM = red maple; RO = red oak; SM = sugar maple; YB = yellow birch.

Table C.1
Sensitivity analysis of parameter estimates in the Spe-CN model. Changes in output variables due to a 20% change in each parameter value are categorized as follows: L (low) < 10%, M (moderate) = 10–30%, H (high) > 30%. Changes > 30% are indicated in bold. Tables A.1 and A.2 describe and list estimates for each parameter. Changes in parameters not included here had no effect on these output variables.

Parameter	NPP				Plant C				Plant N				OeOa C				OeOa C:N				OeOa nitrification				Leaching			
	−20%		+20%		−20%		+20%		−20%		+20%		−20%		+20%		−20%		+20%		−20%		+20%		−20%		+20%	
Production																												
AngioANPPslope	–	M	+	L	–	L	+	L	–	L	–	L	–	M	+	L	–	L	+	L	+	**H**	–	**H**	+	M	–	M
AngioANPPint	+	L	–	L	+	L	–	L	–	L	+	L	+	L	–	L	–	L	–	L	–	M	+	M	–	L	+	L
GymnoANPPslope	–	M	+	M	–	M	+	L	–	L	–	L	–	M	+	M	–	L	+	L	+	L	–	M	+	M	–	L
GymnoANPPint	+	L	–	L	+	L	–	L	–	L	–	L	+	L	–	L	+	L	–	L	–	L	+	L	–	L	+	L
MinFolNCon	–	M	+	L	–	M	+	L	–	L	+	L	–	M	+	L	–	L	+	L	+	**H**	–	**H**	+	M	–	M
FolNConRange	–	L	+	L	–	L	+	L	+	L	–	L	–	L	+	L	+	L	–	L	+	L	–	L	+	L	–	L
MinRootNCon	+	L	–	L	+	L	–	L	+	L	–	L	+	L	–	L	+	L	–	L	–	M	+	L	–	L	–	L
MinFineWoodNcon	–	L	+	L	+	L	–	L	–	L	+	L	+	L	–	L	+	L	–	L	–	L	+	M	–	L	+	L
MinCoarseWood Ncon	+	L	–	L	+	L	–	L	–	L	+	L	+	L	–	L	–	L	–	L	+	M	–	M	+	L	–	L
Allocation and biomass																												
FolAllocAngioA	–	L	+	L	–	L	+	L	–	L	+	L	–	L	+	L	–	L	+	L	+	L	–	L	–	L	–	L
FolAllocAngioB	+	L	–	L	+	M	–	M	+	L	–	M	+	L	–	L	+	L	–	L	–	M	+	M	–	L	–	L
RootProdFracAngio	–	L	+	L	+	L	–	L	+	L	–	L	–	L	+	L	+	L	–	L	+	M	–	**H**	+	L	–	M
FolAllocGymnoA	+	L	–	L	+	L	–	L	+	L	–	L	+	L	–	L	+	L	–	L	–	L	+	L	–	L	+	L
RootProdFracGym	+	L	+	L	+	L	–	L	+	L	–	L	+	L	+	L	+	L	–	L	+	L	–	L	–	L	+	L
CWDFrac	–	L	+	L	–	L	+	L	–	L	+	L	+	M	–	M	+	L	–	L	–	M	+	**H**	–	L	+	L
RootCWDFrac	–	L	+	L	–	L	+	L	–	L	+	L	–	L	+	L	–	L	+	L	–	L	+	L	–	L	+	L
NomMaxWoodC	+	L	–	L	–	L	+	L	–	L	+	L	+	L	–	L	+	L	–	L	+	L	–	L	+	L	–	L
Litterfall and decomposition																												
FolTurnover	–	L	+	L	–	L	+	L	+	L	–	L	–	L	+	L	–	L	+	L	–	L	+	L	–	L	+	L
RootTurnA	+	L	–	L	–	L	+	L	–	L	+	M	+	L	–	L	–	L	+	L	+	L	–	M	+	L	–	L
RootTurnB	–	L	+	L	+	L	–	L	+	L	–	L	–	L	+	L	+	L	–	L	–	L	+	L	–	L	+	L
RootTurnInt	–	L	+	L	+	L	–	L	+	L	–	L	–	L	+	L	–	L	–	L	–	L	+	L	–	L	+	L
FineWoodTurnover	–	L	+	L	+	L	–	L	+	L	–	L	–	L	+	L	–	L	+	L	–	L	+	L	–	L	+	L
NewDeadFine WoodTurn	–	L	+	L	+	L	–	L	–	L	+	L	–	L	+	L	–	L	+	L	–	L	+	L	–	L	+	L
NewDeadCoarse WoodTurn	+	L	–	L	–	L	+	L	+	L	–	L	+	L	+	L	–	L	+	L	+	L	–	L	+	L	–	L
kFragCWD	–	L	+	L	–	L	+	L	–	L	+	L	–	L	+	L	–	L	+	L	+	L	–	L	+	L	–	L
CoarseWoodk	+	L	–	L	–	L	+	L	–	L	–	L	+	L	–	L	+	L	–	L	+	L	–	L	+	L	–	L
NGRatioCWD	+	L	–	L	–	L	–	L	+	L	–	L	–	L	+	L	–	L	+	L	+	L	–	L	+	L	–	L
FolLigCon	+	L	–	L	+	L	–	L	+	L	–	L	–	L	+	L	–	L	+	L	+	L	–	L	+	L	–	L
RootLigCon	+	L	–	L	+	L	–	L	+	L	–	L	–	L	+	L	–	L	+	L	+	M	–	M	+	L	–	L
FineWoodLigCon	+	L	–	L	+	L	–	L	+	L	–	L	–	L	+	L	–	L	+	L	+	M	–	M	+	L	–	L
CoarseWoodLigCon	+	L	–	L	+	L	–	L	+	L	–	L	+	L	+	L	+	L	–	L	+	L	–	L	+	L	–	L
Lignink	–	L	+	L	–	L	+	L	–	L	+	L	+	L	–	L	+	L	–	L	–	L	+	L	–	L	+	L
Cellulosek	–	L	+	L	–	L	+	L	–	L	+	L	+	L	–	L	+	L	–	L	–	M	+	L	–	L	+	L
NLAk	–	L	+	L	–	L	+	L	–	L	+	L	+	L	–	L	+	L	–	L	–	M	+	L	–	L	+	L
CDI	–	L	+	L	–	L	+	L	–	L	+	L	+	L	–	L	+	L	–	L	–	M	+	M	–	L	+	L
FolNML	+	L	–	L	+	L	–	L	+	L	–	L	+	L	–	L	+	L	–	L	+	L	–	L	+	L	–	L
RootNML	+	L	–	L	+	L	–	L	+	L	–	L	+	L	–	L	+	L	–	L	+	L	–	L	+	L	–	L
FineWoodNML	+	L	–	L	+	L	–	L	+	L	–	L	+	L	–	L	+	L	–	L	+	L	–	L	+	L	–	L
CoarseWoodNML	+	L	–	L	+	L	–	L	+	L	–	L	+	L	–	L	+	L	–	L	+	L	–	L	+	L	–	L
Resorp	+	L	–	L	+	L	–	L	+	L	–	L	+	L	–	L	+	L	–	L	–	L	–	L	–	L	–	L
CohortPctNMax	+	L	+	L	+	L	+	L	+	L	+	L	+	L	+	L	+	L	+	L	+	L	+	L	+	L	+	L
Humus and mineral soil																												
HumusSpk	–	L	+	L	–	L	+	L	–	M	+	L	+	M	–	M	+	L	–	L	–	**H**	+	**H**	–	M	+	M
kASOM	–	L	+	L	–	L	+	L	–	L	+	L	–	L	+	L	–	L	+	L	–	L	+	L	–	L	+	L
kPSOM	–	L	+	L	–	L	+	L	–	L	+	L	–	L	+	L	–	L	–	L	–	**H**	+	M	–	M	+	M
HSOMTran	+	L	–	L	+	L	–	L	+	L	–	L	+	L	–	L	–	L	+	L	+	M	–	**H**	+	M	–	M
PSOMFrac	+	L	–	L	+	L	–	L	+	L	–	L	+	L	–	L	–	L	–	L	+	M	–	**H**	+	M	–	M
HumusNGR	–	L	+	L	–	L	+	L	–	M	+	L	–	L	+	L	–	M	+	M	–	**H**	+	M	–	M	+	L
SOMNGR	–	L	+	L	–	L	+	L	–	L	+	L	–	L	+	L	–	L	–	L	–	**H**	+	M	–	M	+	L
MycoNFrac	–	L	+	L	–	L	+	L	–	L	+	L	–	L	+	L	–	L	+	L	+	L	–	L	–	L	+	L
MiningMax	–	L	+	L	–	L	+	L	–	L	+	L	+	L	–	L	+	L	–	L	–	M	+	M	–	L	+	L
Nitrification and leaching																												
NitfracFFslope	–	L	+	L	–	L	+	L	–	L	+	L	–	L	+	L	–	L	–	L	+	L	–	M	–	L	–	L
NitfracFFint	+	L	–	L	+	L	–	L	+	L	–	L	+	L	–	L	–	L	–	L	–	**H**	+	M	–	M	–	L
NitfracSOMslope	–	L	+	L	–	L	+	L	–	L	+	L	–	L	+	L	–	L	+	L	–	L	+	L	+	L	–	L
NitfracSOMint	+	L	–	L	+	L	–	L	+	L	–	L	+	L	–	L	+	L	–	L	+	L	–	L	–	L	+	L
MinNitFraction	+	L	–	L	+	L	–	L	+	L	–	L	+	L	–	L	+	L	–	L	+	L	–	L	+	L	–	L
N deposition																												
NDepNO3frac	+	L	–	L	+	L	–	L	+	L	–	L	+	L	–	L	–	L	+	L	+	M	–	M	–	L	+	L
NdepNO3SoilFrac	–	L	+	L	–	L	+	L	–	L	+	L	–	L	+	L	+	L	–	L	–	L	+	L	+	L	–	L
NdepNO3LitterFrac	–	L	+	L	–	L	+	L	–	L	+	L	–	L	+	L	–	L	+	L	–	L	+	L	–	L	+	L
NdepNH4SoilFrac	+	L	–	L	+	L	–	L	+	L	–	L	+	L	–	L	+	L	–	L	+	L	–	L	+	L	–	L
NdepNH4LitterFrac	–	L	+	L	–	L	+	L	–	L	+	L	–	L	+	L	–	L	+	L	–	L	+	L	–	L	+	L

Field data for productivity and N cycling processes in plots dominated by single species were limited, but Spe-CN model simulations were in general agreement with the available data (Figs. 3 and B.1). For ANPP for the Catskills, Spe-CN modeled values were within two standard errors of the mean field data estimates for hemlock, sugar maple, and oak, and beech was close (Fig. 3). The model overestimated ANPP for yellow birch, however, likely due (as for the soils) to the occurrence of these yellow birch stands over a rock substrate, which may have limited ANPP. The Spe-CN model also slightly underestimated foliar NPP for red oak and sugar maple relative to the field data, suggesting a potential need to improve parameterization determining allocation among plant tissues. Alternatively, the underestimation of foliar NPP for these species may derive from a slight underestimation of foliar N (Fig. B.1), which determines NPP in the model.

For the ratio of nitrification to N mineralization for the OeOa horizons in the forest floor, the Spe-CN model captured the pattern observed among tree species in the Catskills (i.e., maple > beech, yellow birch > hemlock, red oak; Fig. B.1; Lovett et al., 2004). We could not compare Spe-CN modeled values for the OeOa directly to nitrification and N mineralization measurements from GMF because Finzi et al. (1998) did not separate the forest floor and mineral soil in making their measurements. General patterns were similar between Spe-CN simulations and species effects at GMF, however (e.g., maple > beech, oak), with the exception of hemlock, for which the measured nitrification/mineralization ratio was higher than observed in the Catskills (Finzi et al., 1998; Lovett et al., 2004). While the patterns of species effects on OeOa nitrification relative to N mineralization were similar between the field data and the model, the magnitude of the field values was much higher for sugar maple and beech in the Catskills plots than was simulated by Spe-CN (Fig. B.1). The Spe-CN modeled values corresponded well to the WMNF field data, however (Goodale and Aber, 2001; Ollinger et al., 2002).

Appendix C. Sensitivity analysis for parameter estimates

We performed a sensitivity analysis on the full set of parameters employed in the Spe-CN model (Tables A.1 and A.2) to assess the magnitude of change that a 20% increase or decrease in each parameter would generate in key output variables, with all other parameters held constant. The majority of the sensitivity analysis presented here is from model runs for a hypothetical second-growth sugar maple stand in the Catskills, following 80% harvest and 90% removal of aboveground biomass 90 years previously. The analysis for the four gymnosperm-specific parameters derives from hemlock simulations with the same disturbance settings. Sensitivity analyses for the other species included in our invasion simulations showed similar patterns to those for sugar maple (data not shown).

We examined the responses of NPP, plant C, plant N, OeOa C, C:N, and nitrification rates, and NO_3^- leaching to changes in model parameters. Changes of 20% in most parameters had a small effect (<10% change) on most output variables (Table C.1).

As expected, for NPP the most influential parameters were minimum foliar N concentration (MinFolNCon) and the slope of the relationship between foliar N and ANPP (AngioANPPslope or GymnoANPPslope; Tables A.1 and C.1). A 20% change in the value of these parameters caused a moderate (10–30%) change in NPP. Plant C responded similarly to these parameters and also to changes in the intercept of the relationship between foliar N and foliar allocation of ANPP (FolAllocAngioB). In contrast to plant C, plant N had low sensitivity to the parameters governing NPP. Like plant C, plant N showed moderate sensitivity to parameters determining allocation, and was also sensitive to changes in parameters for root turnover (RootTurnA) and humus decomposition (HumusSpk, HumusNGR), which influence availability of N for plant uptake (Table C.1).

For OeOa C, the most influential parameters (still with moderate effect) were those governing NPP, the coarse wood fraction of total wood litter (CWDfrac), and the humus decomposition constant. In contrast, OeOa C:N responded most to changes in the HumusNGR. A decrease in HumusNGR decreased net N mineralization, thereby increasing soil N retention and lowering OeOa C:N.

The output variable with the greatest sensitivity to changes in parameter values was OeOa nitrification, which was the only variable to show a large response (>30%) to a 20% change in some parameters (Table C.1). Levels of OeOa nitrification showed moderate or high sensitivity to changes in parameters governing NPP; minimum N concentrations of foliage, wood, and roots; allocation parameters; root turnover parameters; root and fine wood lignin concentrations; the Climate Decomposition Index (CDI); and most of the decomposition constants and transfer fractions associated with the forest floor and soil organic matter (SOM) pools (Table C.1). This sensitivity to multiple model parameters reflects the dependence of nitrification rates on the outcome of numerous other interacting processes related to both vegetation and soils.

Despite the sensitivity of nitrification rates to changes in many model parameters, NO_3^- leaching responded strongly to changes only in parameters determining NPP, root allocation, and humus and SOM decomposition and transfer among soil pools (Table C.1). Nitrate leaching was generally less sensitive than nitrification to parameter changes because much of the NO_3^- generated during nitrification was taken up by vegetation before it could be leached from the system.

References

Aber, J.D., Driscoll, C.T., 1997. Effects of land use, climate variation, and N deposition on N cycling and C storage in northern hardwood forests. Glob. Biogeochem. Cycles 11, 639–648.

Aber, J.D., Federer, C.A., 1992. A generalized, lumped-parameter model of photosynthesis, evapotranspiration and net primary production in temperate and boreal forest ecosystems. Oecologia 92, 463–474.

Aber, J.D., Melillo, J.M., 1982. Nitrogen immobilization in decaying hardwood leaf litter as a function of initial nitrogen and lignin content. Can. J. Bot. – Rev. Can. De Bot. 60, 2263–2269.

Aber, J.D., Melillo, J.M., McClaugherty, C.A., 1990. Predicting long-term patterns of mass-loss, nitrogen dynamics, and soil organic-matter formation from initial fine litter chemistry in temperate forest ecosystems. Can. J. Bot. – Rev. Can. De Bot. 68, 2201–2208.

Aber, J.D., Melillo, J.M., Nadelhoffer, K.J., McClaugherty, C.A., Pastor, J., 1985. Fine root turnover in forest ecosystems in relation to quantity and form of nitrogen availability – a comparison of two methods. Oecologia 66, 317–321.

Aber, J.D., Ollinger, S.V., Driscoll, C.T., 1997. Modeling nitrogen saturation in forest ecosystems in response to land use and atmospheric deposition. Ecol. Model. 101, 61–78.

Aber, J.D., Ollinger, S.V., Federer, C.A., Reich, P.B., Goulden, M.L., Kicklighter, D.W., Melillo, J.M., Lathrop, R.G., 1995. Predicting the effects of climate change on water yield and forest production in the northeastern United States. Clim. Res. 5, 207–222.

Alban, D.H., Pastor, J., 1993. Decomposition of aspen, spruce, and pine boles on 2 sites in Minnesota. Can. J. For. Res. – Rev. Can. De Rech. Forest. 23, 1744–1749.

Albani, M., Moorcroft, P.R., Ellison, A.M., Orwig, D.A., Foster, D.R., 2010. Predicting the impact of hemlock woolly adelgid on carbon dynamics of eastern United States forests. Can. J. For. Res. – Rev. Can. De Rech. Forest. 40, 119–133.

Aukema, J.E., McCullough, D.G., Von Holle, B., Liebhold, A.M., Britton, K., Frankel, S.J., 2010. Historical accumulation of nonindigenous forest pests in the continental United States. Bioscience 60, 886–897.

Averill, C., Turner, B.L., Finzi, A.C., 2014. Mycorrhiza-mediated competition between plants and decomposers drives soil carbon storage. Nature 505, 543–545.

Baskerville, G.L., 1965. Estimation of dry weight of tree components and total standing crop in conifer stands. Ecology 46, 867–869.

Berg, B., 2014. Decomposition patterns for foliar litter – a theory for influencing factors. Soil Biol. Biochem. 78, 222–232.

Berntson, G.M., Aber, J.D., 2000. Fast nitrate immobilization in N saturated temperate forest soils. Soil Biol. Biochem. 32, 151–156.

Binkley, D., Menyailo, O. (Eds.), 2005. Tree Species Effects on Soils: Implications for Global Change. Springer, Netherlands.
Bockheim, J.G., Jepsen, E.A., Heisey, D.M., 1991. Nutrient dynamics in decomposing leaf litter of 4 tree species on a sandy soil in northwestern Wisconsin. Can. J. For. Res. – Rev. Can. De Rech. Forest. 21, 803–812.
Boerner, R.E.J., 1984. Foliar nutrient dynamics and nutrient use efficiency of 4 deciduous tree species in relation to site fertility. J. Appl. Ecol. 21, 1029–1040.
Boerner, R.E.J., Rebbeck, J., 1995. Decomposition and nitrogen release from leaves of 3 hardwood species grown under elevated O_3 and/or CO_2. Plant Soil 170, 149–157.
Campbell, J., Bailey, A., 2015a. Hubbard Brook Experimental Forest: Daily Mean Temperature Data, 1955 – Present. Hubbard Brook Data Archive [Database]. <http://www.hubbardbrook.org/data/dataset.php?id=58>.
Campbell, J., Bailey, A., 2015b. Hubbard Brook Experimental Forest: Total Daily Precipitation by Watershed, 1956 – Present. Hubbard Brook Data Archive [Database]. <http://www.hubbardbrook.org/data/dataset.php?id=14>.
Campbell, J.L., Gower, S.T., 2000. Detritus production and soil N transformations in old-growth eastern hemlock and sugar maple stands. Ecosystems 3, 185–192.
Canham, C.D., Rogers, N., Buchholz, T., 2013. Regional variation in forest harvest regimes in the northeastern United States. Ecol. Appl. 23, 515–522.
Cobb, R.C., 2010. Species shift drives decomposition rates following invasion by hemlock woolly adelgid. Oikos 119, 1291–1298.
Cobb, R.C., Chan, M.N., Meentemeyer, R.K., Rizzo, D.M., 2012. Common factors drive disease and coarse woody debris dynamics in forests impacted by sudden oak death. Ecosystems 15, 242–255.
Cobb, R.C., Eviner, V.T., Rizzo, D.M., 2013. Mortality and community changes drive sudden oak death impacts on litterfall and soil nitrogen cycling. New Phytol. 200, 422–431.
Colman, B.P., Fierer, N., Schimel, J.P., 2008. Abiotic nitrate incorporation, anaerobic microsites, and the ferrous wheel. Biogeochemistry 91, 223–227.
Cools, N., Vesterdal, L., De Vos, B., Vanguelova, E., Hansen, K., 2014. Tree species is the major factor explaining C:N ratios in European forest soils. For. Ecol. Manage. 311, 3–16.
Cornwell, W.K., Weedon, J.T., 2014. Decomposition trajectories of diverse litter types: a model selection analysis. Methods Ecol. Evol. 5, 173–182.
Dail, D.B., Davidson, E.A., Chorover, J., 2001. Rapid abiotic transformation of nitrate in an acid forest soil. Biogeochemistry 54, 131–146.
Demers, J.D., Driscoll, C.T., Fahey, T.J., Yavitt, J.B., 2007. Mercury cycling in litter and soil in different forest types in the Adirondack region, New York, USA. Ecol. Appl. 17, 1341–1351.
Dietze, M.C., Matthes, J.H., 2014. A general ecophysiological framework for modelling the impact of pests and pathogens on forest ecosystems. Ecol. Lett. 17, 1418–1426.
Downs, M.R., Nadelhoffer, K.J., Melillo, J.M., Aber, J.D., 1996. Immobilization of a N-15-labeled nitrate addition by decomposing forest litter. Oecologia 105, 141–150.
Ellison, A.M., Bank, M.S., Clinton, B.D., Colburn, E.A., Elliott, K., Ford, C.R., Foster, D.R., Kloeppel, B.D., Knoepp, J.D., Lovett, G.M., Mohan, J., Orwig, D.A., Rodenhouse, N. L., Sobczak, W.V., Stinson, K.A., Stone, J.K., Swan, C.M., Thompson, J., Von Holle, B., Webster, J.R., 2005. Loss of foundation species: consequences for the structure and dynamics of forested ecosystems. Front. Ecol. Environ. 3, 479–486.
Fahey, T.J., Hughes, J.W., Pu, M., Arthur, M.A., 1988. Root decomposition and nutrient flux following whole-tree harvest of northern hardwood forest. For. Sci. 34, 744–768.
Fahey, T.J., Siccama, T.G., Driscoll, C.T., Likens, G.E., Campbell, J., Johnson, C.E., Battles, J.J., Aber, J.D., Cole, J.J., Fisk, M.C., Groffman, P.M., Hamburg, S.P., Holmes, R.T., Schwarz, P.A., Yanai, R.D., 2005. The biogeochemistry of carbon at Hubbard Brook. Biogeochemistry 75, 109–176.
Finzi, A.C., Raymer, P.C.L., Giasson, M.A., Orwig, D.A., 2014. Net primary production and soil respiration in New England hemlock forests affected by the hemlock woolly adelgid. Ecosphere 5 (8) 98.
Finzi, A.C., Van Breemen, N., Canham, C.D., 1998. Canopy tree soil interactions within temperate forests: species effects on soil carbon and nitrogen. Ecol. Appl. 8, 440–446.
Fitzhugh, R.D., Lovett, G.M., Venterea, R.T., 2003. Biotic and abiotic immobilization of ammonium, nitrite, and nitrate in soils developed under different tree species in the Catskill Mountains, New York, USA. Glob. Change Biol. 9, 1591–1601.
Foster, J.R., Lang, G.E., 1982. Decomposition of red spruce and balsam fir boles in the White Mountains of New Hampshire. Can. J. For. Res. – Rev. Can. De Rech. Forest. 12, 617–626.
Freschet, G.T., Cornwell, W.K., Wardle, D.A., Elumeeva, T.G., Liu, W.D., Jackson, B.G., Onipchenko, V.G., Soudzilovskaia, N.A., Tao, J.P., Cornelissen, J.H.C., 2013. Linking litter decomposition of above- and below-ground organs to plant-soil feedbacks worldwide. J. Ecol. 101, 943–952.
Gartner, T.B., Cardon, Z.G., 2006. Site of leaf origin affects how mixed litter decomposes. Soil Biol. Biochem. 38, 2307–2317.
Goodale, C.L., Aber, J.D., 2001. The long-term effects of land-use history on nitrogen cycling in northern hardwood forests. Ecol. Appl. 11, 253–267.
Gosz, J.R., Likens, G.E., Bormann, F.H., 1973. Nutrient release from decomposing leaf and branch litter in the Hubbard Brook forest, New Hampshire. Ecol. Monogr. 42, 173–191.
Gower, S.T., Reich, P.B., Son, Y., 1993. Canopy dynamics and aboveground production of 5 tree species with different leaf longevities. Tree Physiol. 12, 327–345.
Gower, S.T., Son, Y., 1992. Differences in soil and leaf litterfall nitrogen dynamics for 5 forest plantations. Soil Sci. Soc. Am. J. 56, 1959–1966.
Griffin, J.M., Turner, M.G., 2012. Changes to the N cycle following bark beetle outbreaks in two contrasting conifer forest types. Oecologia 170, 551–565.
Hancock, J.E., Arthur, M.A., Weathers, K.C., Lovett, G.M., 2008. Carbon cycling along a gradient of beech bark disease impact in the Catskill Mountains, New York. Can. J. For. Res. – Rev. Can. De Rech. Forest. 38, 1267–1274.
Hicke, J.A., Allen, C.D., Desai, A.R., Dietze, M.C., Hall, R.J., Hogg, E.H., Kashian, D.M., Moore, D., Raffa, K.F., Sturrock, R.N., Vogelmann, J., 2012. Effects of biotic disturbances on forest carbon cycling in the United States and Canada. Glob. Change Biol. 18, 7–34.
Hobara, S., Tokuchi, N., Ohte, N., Koba, K., Katsuyama, M., Kim, S.J., Nakanishi, A., 2001. Mechanism of nitrate loss from a forested catchment following a small-scale, natural disturbance. Can. J. For. Res. – Rev. Can. De Rech. Forest. 31, 1326–1335.
Hobbie, S.E., 1992. Effects of plant species on nutrient cycling. Trends Ecol. Evol. 7, 336–339.
Hobbie, S.E., 2005. Contrasting effects of substrate and fertilizer nitrogen on the early stages of litter decomposition. Ecosystems 8, 644–656.
Hobbie, S.E., 2015. Plant species effects on nutrient cycling: revisiting litter feedbacks. Trends Ecol. Evol. 30, 357–363.
Hobbie, S.E., Oleksyn, J., Eissenstat, D.M., Reich, P.B., 2010. Fine root decomposition rates do not mirror those of leaf litter among temperate tree species. Oecologia 162, 505–513.
Hobbie, S.E., Reich, P.B., Oleksyn, J., Ogdahl, M., Zytkowiak, R., Hale, C., Karolewski, P., 2006. Tree species effects on decomposition and forest floor dynamics in a common garden. Ecology 87, 2288–2297.
Houston, D.R., 1994. Major new tree disease epidemics – beech bark disease. Annu. Rev. Phytopathol. 32, 75–87.
Ireland, K.B., Hardy, G.E.S., Kriticos, D.J., 2013. Combining inferential and deductive approaches to estimate the potential geographical range of the invasive plant pathogen, *Phytophthora ramorum*. Plos One 8 (5), e63508.
Iverson, L.R., Prasad, A.M., Matthews, S.N., 2008a. Modeling potential climate change impacts on the trees of the northeastern United States. Mitig. Adapt. Strat. Glob. Change 13, 487–516.
Iverson, L.R., Prasad, A.M., Matthews, S.N., Peters, M., 2008b. Estimating potential habitat for 134 eastern US tree species under six climate scenarios. For. Ecol. Manage. 254, 390–406.
Jenkins, J.C., Aber, J.D., Canham, C.D., 1999. Hemlock woolly adelgid impacts on community structure and N cycling rates in eastern hemlock forests. Can. J. For. Res. – Rev. Can. De Rech. Forest. 29, 630–645.
Johnson, C.E., 2013. Chemical properties of upland forest soils in the Catskills region. Ann. N. Y. Acad. Sci. 1298, 30–42.
Kaczmarek, D.J., Pope, P.E., Scott, D.A., Idol, T., 1998. Foliar and belowground nutrient dynamics in mixed hardwood forest ecosystems. USDA Forest Service, Southern Research Station, Asheville, NC, pp. 129–135.
Kudish, M., 1979. Catskills Soils and Forest History. Catskill Center for Conservation and Development Inc, Hobart, NY.
Lambert, R.L., Lang, G.E., Reiners, W.A., 1980. Loss of mass and chemical change in decaying boles of a subalpine balsam fir forest. Ecology 61, 1460–1473.
Langley, J.A., Hungate, B.A., 2003. Mycorrhizal controls on belowground litter quality. Ecology 84, 2302–2312.
Lewis, D.B., Castellano, M.J., Kaye, J.P., 2014. Forest succession, soil carbon accumulation, and rapid nitrogen storage in poorly remineralized soil organic matter. Ecology 95, 2687–2693.
Liebhold, A.M., McCullough, D.G., Blackburn, L.M., Frankel, S.J., Von Holle, B., Aukema, J.E., 2013. A highly aggregated geographical distribution of forest pest invasions in the USA. Divers. Distrib. 19, 1208–1216.
Loo, J., 2009. Ecological impacts of non-indigenous invasive fungi as forest pathogens. Biol. Invasions 11, 81–96.
Lovett, G.M., Arthur, M.A., Crowley, K.F., 2015. Effects of calcium on the rate and extent of litter decomposition in a Northern Hardwood forest. Ecosystems.
Lovett, G.M., Arthur, M.A., Weathers, K.C., Fitzhugh, R.D., Templer, P.H., 2013a. Nitrogen addition increases carbon storage in soils, but not in trees, in an eastern US deciduous forest. Ecosystems 16, 980–1001.
Lovett, G.M., Arthur, M.A., Weathers, K.C., Griffin, J.M., 2010. Long-term changes in forest carbon and nitrogen cycling caused by an introduced pest/pathogen complex. Ecosystems 13, 1188–1200.
Lovett, G.M., Arthur, M.A., Weathers, K.C., Griffin, J.M., 2013b. Effects of introduced insects and diseases on forest ecosystems in the Catskill Mountains of New York. Ann. N. Y. Acad. Sci. 1298, 66–77.
Lovett, G.M., Bowser, J.J., Edgerton, E.S., 1997. Atmospheric deposition to watersheds in complex terrain. Hydrol. Process. 11, 645–654.
Lovett, G.M., Canham, C.D., Arthur, M.A., Weathers, K.C., Fitzhugh, R.D., 2006. Forest ecosystem responses to exotic pests and pathogens in eastern North America. Bioscience 56, 395–405.
Lovett, G.M., Rueth, H., 1999. Soil nitrogen transformations in beech and maple stands along a nitrogen deposition gradient. Ecol. Appl. 9, 1330–1344.
Lovett, G.M., Weathers, K.C., Arthur, M.A., 2002. Control of nitrogen loss from forested watersheds by soil carbon: nitrogen ratio and tree species composition. Ecosystems 5, 712–718.
Lovett, G.M., Weathers, K.C., Arthur, M.A., Schultz, J.C., 2004. Nitrogen cycling in a northern hardwood forest: do species matter? Biogeochemistry 67, 289–308.
Lovett, G.M., Weathers, K.C., Sobczak, W.V., 2000. Nitrogen saturation and retention in forested watersheds of the Catskill Mountains, New York. Ecol. Appl. 10, 73–84.

Macmillan, P.C., 1988. Decomposition of coarse woody debris in an old-growth Indiana forest. Can. J. For. Res. – Rev. Can. De Rech. Forest. 18, 1353–1362.
Magill, A.H., Aber, J.D., 1998. Long-term effects of experimental nitrogen additions on foliar litter decay and humus formation in forest ecosystems. Plant Soil 203, 301–311.
Magill, A.H., Aber, J.D., Currie, W.S., Nadelhoffer, K.J., Martin, M.E., McDowell, W.H., Melillo, J.M., Steudler, P., 2004. Ecosystem response to 15 years of chronic nitrogen additions at the Harvard Forest LTER, Massachusetts, USA. For. Ecol. Manage. 196, 7–28.
McClaugherty, C.A., Aber, J.D., Melillo, J.M., 1982. The role of fine roots in the organic-matter and nitrogen budgets of 2 forested ecosystems. Ecology 63, 1481–1490.
McClaugherty, C.A., Aber, J.D., Melillo, J.M., 1984. Decomposition dynamics of fine roots in forested ecosystems. Oikos 42, 378–386.
McFarlane, K.J., Torn, M.S., Hanson, P.J., Porras, R.C., Swanston, C.W., Callaham Jr., M. A., Guilderson, T.P., 2013. Comparison of soil organic matter dynamics at five temperate deciduous forests with physical fractionation and radiocarbon measurements. Biogeochemistry 112, 457–476.
Melillo, J.M., Aber, J.D., Muratore, J.F., 1982. Nitrogen and lignin control of hardwood leaf litter decomposition dynamics. Ecology 63, 621–626.
Millard, P., Grelet, G.A., 2010. Nitrogen storage and remobilization by trees: ecophysiological relevance in a changing world. Tree Physiol. 30, 1083–1095.
Moorcroft, P.R., Hurtt, G.C., Pacala, S.W., 2001. A method for scaling vegetation dynamics: the ecosystem demography model (ED). Ecol. Monogr. 71, 557–585.
Morin, R.S., Liebhold, A.M., 2015. Invasions by two non-native insects alter regional forest species composition and successional trajectories. For. Ecol. Manage. 341, 67–74.
Morse, J.L., Duran, J., Beall, F., Enanga, E.M., Creed, I.F., Fernandez, I., Groffman, P.M., 2015. Soil denitrification fluxes from three northeastern North American forests across a range of nitrogen deposition. Oecologia 177, 17–27.
Nadelhoffer, K.J., Downs, M.R., Fry, B., 1999. Sinks for N-15-enriched additions to an oak forest and a red pine plantation. Ecol. Appl. 9, 72–86.
Nadelhoffer, K.J., Downs, M.R., Fry, B., Aber, J.D., Magill, A.H., Melillo, J.M., 1995. The fate of N-15-labeled nitrate additions to a northern hardwood forest in eastern Maine, USA. Oecologia 103, 292–301.
Nadelhoffer, K.J., Raich, J.W., 1992. Fine root production estimates and belowground carbon allocation in forest ecosystems. Ecology 73, 1139–1147.
NERC, 2010. Northeastern Ecosystem Research Cooperative (NERC) Compilation of Foliar Chemistry Data for the Northeastern United States and Southeastern Canada. NERC 12.6 <http://www.nercscience.org>.
Norby, R.J., Long, T.M., Hartz-Rubin, J.S., O'Neill, E.G., 2000. Nitrogen resorption in senescing tree leaves in a warmer, CO_2-enriched atmosphere. Plant Soil 224, 15–29.
Ollinger, S., Aber, J., Federer, C., Lovett, G., Ellis, J., 1995. Modeling physical and chemical climate of the northeastern United States for a geographical information system. In. USDA Forest Service General Technical Report NE-191, Radnor, PA.
Ollinger, S.V., Aber, J.D., Lovett, G.M., Millham, S.E., Lathrop, R.G., Ellis, J.M., 1993. A spatial model of atmospheric deposition for the northeastern United States. Ecol. Appl. 3, 459–472.
Ollinger, S.V., Goodale, C.L., Hayhoe, K., Jenkins, J.P., 2008. Potential effects of climate change and rising CO_2 on ecosystem processes in northeastern US forests. Mitig. Adapt. Strat. Glob. Change 13, 467–485.
Ollinger, S.V., Smith, M.L., Martin, M.E., Hallett, R.A., Goodale, C.L., Aber, J.D., 2002. Regional variation in foliar chemistry and N cycling among forests of diverse history and composition. Ecology 83, 339–355.
Olsson, B.A., Hansson, K., Persson, T., Beuker, E., Helmisaari, H.S., 2012. Heterotrophic respiration and nitrogen mineralisation in soils of Norway spruce, Scots pine and silver birch stands in contrasting climates. For. Ecol. Manage. 269, 197–205.
Orwig, D.A., Cobb, R.C., D'Amato, A.W., Kizlinski, M.L., Foster, D.R., 2008. Multi-year ecosystem response to hemlock woolly adelgid infestation in southern New England forests. Can. J. For. Res. – Rev. Can. De Rech. Forest. 38, 834–843.
Orwig, D.A., Foster, D.R., Mausel, D.L., 2002. Landscape patterns of hemlock decline in New England due to the introduced hemlock woolly adelgid. J. Biogeogr. 29, 1475–1487.
Pacala, S.W., Canham, C.D., Saponara, J., Silander, J.A., Kobe, R.K., Ribbens, E., 1996. Forest models defined by field measurements: estimation, error analysis and dynamics. Ecol. Monogr. 66, 1–43.
Pare, D., Bernier, P., Lafleur, B., Titus, B.D., Thiffault, E., Maynard, D.G., Guo, X.J., 2013. Estimating stand-scale biomass, nutrient contents, and associated uncertainties for tree species of Canadian forests. Can. J. For. Res. – Rev. Can. De Rech. Forest. 43, 599–608.
Park, B.B., Yanai, R.D., Fahey, T.J., Bailey, S.W., Siccama, T.G., Shanley, J.B., Cleavitt, N. L., 2008. Fine root dynamics and forest production across a calcium gradient in northern hardwood and conifer ecosystems. Ecosystems 11, 325–341.
Parsons, W.F.J., Bockheim, J.G., Lindroth, R.L., 2008. Independent, interactive, and species-specific responses of leaf litter decomposition to elevated CO_2 and O-3 in a northern hardwood forest. Ecosystems 11, 505–519.
Parton, W., Silver, W.L., Burke, I.C., Grassens, L., Harmon, M.E., Currie, W.S., King, J.Y., Adair, E.C., Brandt, L.A., Hart, S.C., Fasth, B., 2007. Global-scale similarities in nitrogen release patterns during long-term decomposition. Science 315, 361–364.
Parton, W.J., Schimel, D.S., Cole, C.V., Ojima, D.S., 1987. Analysis of factors controlling soil organic matter levels in Great Plains grasslands. Soil Sci. Soc. Am. J. 51, 1173–1179.
Parton, W.J., Stewart, J.W.B., Cole, C.V., 1988. Dynamics of C, N, P and S in grassland soils – a model. Biogeochemistry 5, 109–131.
Pastor, J., Post, W.M., 1986. Influence of climate, soil moisture, and succession on forest carbon and nitrogen cycles. Biogeochemistry 2, 3–27.
Peltzer, D.A., Allen, R.B., Lovett, G.M., Whitehead, D., Wardle, D.A., 2010. Effects of biological invasions on forest carbon sequestration. Glob. Change Biol. 16, 732–746.
Phillips, R.P., Brzostek, E., Midgley, M.G., 2013. The mycorrhizal-associated nutrient economy: a new framework for predicting carbon–nutrient couplings in temperate forests. New Phytol. 199, 41–51.
Phillips, R.P., Finzi, A.C., Bernhardt, E.S., 2011. Enhanced root exudation induces microbial feedbacks to N cycling in a pine forest under long-term CO_2 fumigation. Ecol. Lett. 14, 187–194.
Piatek, K.B., Munasinghe, P., Peterjohn, W.T., Adams, M.B., Cumming, J.R., 2009. Oak contribution to litter nutrient dynamics in an Appalachian forest receiving elevated nitrogen and dolomite. Can. J. For. Res. – Rev. Can. De Rech. Forest. 39, 936–944.
Polyakova, O., Billor, N., 2007. Impact of deciduous tree species on litterfall quality, decomposition rates and nutrient circulation in pine stands. For. Ecol. Manage. 253, 11–18.
Pouyat, R.V., Carreiro, M.M., 2003. Controls on mass loss and nitrogen dynamics of oak leaf litter along an urban-rural land-use gradient. Oecologia 135, 288–298.
Pregitzer, K.S., Burton, A.J., Mroz, G.D., Liechty, H.O., Macdonald, N.W., 1992. Foliar sulfur and nitrogen along an 800-km pollution gradient. Can. J. For. Res. – Rev. Can. De Rech. Forest. 22, 1761–1769.
Pregitzer, K.S., Burton, A.J., Zak, D.R., Talhelm, A.F., 2008. Simulated chronic nitrogen deposition increases carbon storage in Northern Temperate forests. Glob. Change Biol. 14, 142–153.
Prescott, C.E., 2010. Litter decomposition: what controls it and how can we alter it to sequester more carbon in forest soils? Biogeochemistry 101, 133–149.
Raymer, P.C.L., Orwig, D.A., Finzi, A.C., 2013. Hemlock loss due to the hemlock woolly adelgid does not affect ecosystem C storage but alters its distribution. Ecosphere 4 (5) 63.
Reich, P.B., Oleksyn, J., Modrzynski, J., Mrozinski, P., Hobbie, S.E., Eissenstat, D.M., Chorover, J., Chadwick, O.A., Hale, C.M., Tjoelker, M.G., 2005. Linking litter calcium, earthworms and soil properties: a common garden test with 14 tree species. Ecol. Lett. 8, 811–818.
Rizzo, D.M., Garbelotto, M., Hansen, E.A., 2005. *Phytophthora ramorum*: integrative research and management of an emerging pathogen in California and Oregon forests. Annu. Rev. Phytopathol. 43, 309–335.
Rodriguez, A., Lovett, G.M., Weathers, K.C., Arthur, M.A., Templer, P.H., Goodale, C.L., Christenson, L.M., 2014. Lability of C in temperate forest soils: assessing the role of nitrogen addition and tree species composition. Soil Biol. Biochem. 77, 129–140.
Ross, D.S., Bailey, S.W., Lawrence, G.B., Shanley, J.B., Fredriksen, G., Jamison, A.E., Brousseau, P.A., 2011. Near-surface soil carbon, carbon/nitrogen ratio, and tree species are tightly linked across northeastern United States watersheds. For. Sci. 57, 460–469.
Rustad, L.E., 1994. Element dynamics along a decay continuum in a red spruce ecosystem in Maine, USA. Ecology 75, 867–879.
Scheibe, A., Steffens, C., Seven, J., Jacob, A., Hertel, D., Leuschner, C., Gleixner, G., 2015. Effects of tree identity dominate over tree diversity on the soil microbial community structure. Soil Biol. Biochem. 81, 219–227.
Smith, K.T., Shortle, W.C., Jellison, J., Connolly, J., Schilling, J., 2007. Concentrations of Ca and Mg in early stages of sapwood decay in red spruce, eastern hemlock, red maple, and paper birch. Can. J. For. Res. – Rev. Can. De Rech. Forest. 37, 957–965.
Smith, M.L., Ollinger, S.V., Martin, M.E., Aber, J.D., Hallett, R.A., Goodale, C.L., 2002. Direct estimation of aboveground forest productivity through hyperspectral remote sensing of canopy nitrogen. Ecol. Appl. 12, 1286–1302.
Sprugel, D.G., 1984. Density, biomass, productivity, and nutrient cycling changes during stand development in wave-regenerated balsam fir forests. Ecol. Monogr. 54, 165–186.
Stadler, B., Muller, T., Orwig, D., Cobb, R., 2005. Hemlock woolly adelgid in New England forests: canopy impacts transforming ecosystem processes and landscapes. Ecosystems 8, 233–247.
Strukelj, M., Brais, S., Quideau, S.A., Oh, S.W., 2012. Chemical transformations of deadwood and foliar litter of mixed boreal species during decomposition. Can. J. For. Res. – Rev. Can. De Rech. Forest. 42, 772–788.
Templer, P.H., Lovett, G.M., Weathers, K.C., Findlay, S.E., Dawson, T.E., 2005. Influence of tree species on forest nitrogen retention in the Catskill Mountains, New York, USA. Ecosystems 8, 1–16.
Tonitto, C., Goodale, C.L., Weiss, M.S., Frey, S.D., Ollinger, S.V., 2014. The effect of nitrogen addition on soil organic matter dynamics: a model analysis of the Harvard Forest Chronic Nitrogen Amendment Study and soil carbon response to anthropogenic N deposition. Biogeochemistry 117, 431–454.
Trotter, R.T., Shields, K.S., 2009. Variation in winter survival of the invasive hemlock woolly adelgid (Hemiptera: Adelgidae) across the eastern United States. Environ. Entomol. 38, 577–587.
Tyrrell, L.E., Crow, T.R., 1994. Dynamics of dead wood in old-growth hemlock hardwood forests of northern Wisconsin and northern Michigan. Can. J. For. Res. – Rev. Can. De Rech. Forest. 24, 1672–1683.
Urbanova, M., Snajdr, J., Baldrian, P., 2015. Composition of fungal and bacterial communities in forest litter and soil is largely determined by dominant trees. Soil Biol. Biochem. 84, 53–64.
USFS, 2013. US Forest Service Forest Inventory and Analysis Program Database. FIADB 5.1. USDA USFS <http://fia.fs.fed.us/>.

Vesterdal, L., Elberling, B., Christiansen, J.R., Callesen, I., Schmidt, I.K., 2012. Soil respiration and rates of soil carbon turnover differ among six common European tree species. For. Ecol. Manage. 264, 185–196.

Vesterdal, L., Schmidt, I.K., Callesen, I., Nilsson, L.O., Gundersen, P., 2008. Carbon and nitrogen in forest floor and mineral soil under six common European tree species. For. Ecol. Manage. 255, 35–48.

Whittinghill, K.A., Currie, W.S., Zak, D.R., Burton, A.J., Pregitzer, K.S., 2012. Anthropogenic N deposition increases soil C storage by decreasing the extent of litter decay: analysis of field observations with an ecosystem model. Ecosystems 15, 450–461.

Yorks, T.E., Leopold, D.J., Raynal, D.J., 2003. Effects of *Tsuga canadensis* mortality on soil water chemistry and understory vegetation: possible consequences of an invasive insect herbivore. Can. J. For. Res. – Rev. Can. De Rech. Forest. 33, 1525–1537.

Zak, D.R., Pregitzer, K.S., Host, G.E., 1986. Landscape variation in nitrogen mineralization and nitrification. Can. J. For. Res. – Rev. Can. De Rech. Forest. 16, 1258–1263.